

Analysis of a Split-Path Gear Train with Fluid-Film Bearings

by

Andrew V. Wolff

Thesis submitted to the faculty of the
Virginia Polytechnic Institute and State University
In partial fulfillment of the requirements for the degree of

Master of Science

in

Mechanical Engineering

Committee Members:
R. Gordon Kirk, Chair
Charles Reinholtz
Daniel J. Inman

May 6, 2004
Blacksburg, VA

Keywords: helical, gearbox, split path, split torque

Copyright 2004

Analysis of a Split-Path Gear Train with Fluid-Film Bearings

Andrew Wolff, M.S.

Virginia Polytechnic Institute and State University, 2004

Advisor: R. Gordon Kirk

(Abstract)

In the current literature, split path gear trains are analyzed for use in helicopter transmissions and marine gearboxes. The goal in these systems is to equalize the torque in each path as much as possible. There are other gear trains where the operator intends to hold the torque split unevenly. This allows for control over the gearbox bearing loading which in turn has a direct effect on bearing stiffness and damping characteristics. Having control over these characteristics is a benefit to a designer or operator concerned with suppressing machine vibration.

This thesis presents an analytical method for analyzing the torque in split path gear trains. A computer program was developed that computes the bearing loads in various gearbox arrangements using the torque information gathered by the analytical method. A case study is presented that demonstrates the significance of the analytical method in troubleshooting an industrial gearbox that has excessive vibration.

To my father,
Dr. David A. Wolff,
and my mother,
Dr. Linda D. Wolff

Acknowledgements

I would like to thank my advisor, Dr. Gordon Kirk, for his guidance throughout my graduate work at Virginia Polytechnic Institute and State University. I appreciate the invitation to conduct rotor dynamics research after attending his class on the topic. I would also like to extend my thanks to Dr. Charles Reinholtz and Dr. Daniel J. Inman as members of my advisory committee.

Finally I would like to thank my parents and Jen for their support and love throughout my academic career. It has been rewarding and exciting sharing the graduate student experience with Jen.

Table of Contents

	page
Abstract	ii
Dedication	iii
Acknowledgements	iv
List of Figures	vii
List of Tables	ix
Nomenclature	x
Chapter 1 Introduction	1
1.1 Literature Review.....	2
1.2 Research Objectives.....	4
Chapter 2 Bearing Loads in a Gearbox	5
2.1 Introduction.....	5
2.2 Concepts and Definitions.....	5
2.3 Visual Basic.NET Code	10
Chapter 3 Split Path Gear Trains	16
3.1 Introduction	16
3.2 Concepts and Definitions	16
3.3 Analytical Model	21
3.4 Computer Program Split Path Calculation	28
Chapter 4 Case Study: CRF Test Stand	33
4.1 Introduction	33
4.2 Analytical Model Comparison	41
Chapter 5 Conclusions and Recommendations	50
5.1 Conclusions	50
5.2 Recommendations	51

Table of Contents (continued)

	page
References	53
Appendix A -- Gear Layout 1 Code Segment	54
Appendix B -- Gear Layout 2 Code Segment	58
Appendix C -- Bearing Profile Plotting Program	65
Vita	67

List of Figures

	page
2.1 Helical Gear Nomenclature	7
2.2 Helical Gear Mesh Force Components	8
2.3 Helical Gear Axial Force Directions	9
2.4 Gear Layout Option Screen	10
2.5 Force Vector Diagram for Gear Layout 1	11
2.6 Bearing Location Input Screen for Gear Layout 1	12
2.7 Shaft Mass Input Screen for Gear Layout 1	13
2.8 Gear Parameter Input Screen for Gear Layout 1	14
2.9 Bearing Loads Results Screen for Gear Layout 1	15
3.1 Split Path Gear Train – Front View	18
3.2 Split Path Gear Train – Top View	19
3.3 Conceptual Plot of Split Path Torque	20
3.4 Split Path Torque – Each torque path has identical stiffness	26
3.5 Split Path Torque – Path B has greater stiffness than path A	27
3.6 Split Path Torque – Path A has greater stiffness than path B	27
3.7 Bearing and Gear Arrangement for Gear Layout 2	28
3.8 Force Vector Diagrams for Gear Layout 2	29
3.9 Bearing Location Input Screen for Gear Layout 2	30
3.10 Gear Parameter Input Screen for Gear Layout 2	31
3.11 Bearing Loads Result Screen for Gear Layout 2	32
4.1 CRF Test Stand Gear Train	34
4.2 High Speed Pinion Shaft DyRoBeS Model	36
4.3 Multiple Station Forced Response with estimated bearing loading	36
4.4 High Speed Pinion Shaft Bearing Profile	38
4.5 Matlab plot used to match measured bearing profile	40
4.6 Torque split plot using the CRF gear train parameters	44

List of Figures (continued)

	page
4.7 Torque Split in Path B as a Function of Clocking Angle – CRF gear train parameters	45
4.8 Torque in Each Path using as a Function of Clocking Angle – CRF gear train parameters	45
4.9 BePerf Bearing Diagram Updated with Correct Loading Vector	46
4.10 Multiple Station Forced Response – 10,000 HP	47
4.11 3D Forced Response – 10,000 HP – 0.56 Torque Split	47
4.12 Sensitivity Plot – Changes in Support Stiffness	48
4.13 Sensitivity Plot -- Changes in Torque Splits	49

List of Tables

	page
4.1 Comparison Between DyRoBeS and VT-FAST Software	35
4.2 BePerf Approximate and Improved Bearing Properties	41
4.3 Stiffness Factors in each Path of the CRF test stand	42
4.4 Bearing Support Stiffness Sensitivity	49
4.5 Bearing Load Sensitivity	49

Nomenclature

$ac = p_t$ = transverse circular pitch

$ae = p_n$ = normal circular pitch

C_b = Bearing clearance

C_p = Lobe radial clearance

C_{xx} = Bearing damping in the x-direction

D = Bearing inner diameter

F_a = Helical gear axial force component

F_n = Helical gear transmission force

F_r = Helical gear radial force component

F_t = Helical gear tangential force component

GR = gear reduction ratio of the input pinion and compound shaft gear

k_A = torsional stiffness of path A

k_B = torsional stiffness of path B

K_{xx} = Bearing stiffness in the x-direction

L = Bearing length

L/D = Length to Diameter ratio

LWB = loaded windup of power path B

LWA = loaded windup of power path A

m = slope

$m^{(A)}$ = slope of the line representing path A

$m^{(B)}$ = slope of the line representing path B

P_n = normal diametral pitch

P_t = Transverse Diametral Pitch

p_n = normal circular pitch

p_t = transverse circular pitch

Nomenclature (continued)

T_{in} = Lube oil inlet temperature

Torque Split^(A) = percentage of total torque in path A

Torque Split_B = percentage of total torque in path B

α = offset

β = clocking angle

β_{ini} = initial clocking angle

δ = preload

θ_L = Angle to leading edge of pad

τ = torque

τ_A = torque through path A

τ_B = torque through path B

τ_{total} = total input torque

ϕ_t = transverse pressure angle

ϕ_n = normal pressure angle

χ = Angular extent of lobe

ψ = helix angle

Chapter 1

Introduction

It is common for industrial equipment to utilize a gear train as part of the drive system. The gear train is often composed of one or two gearboxes that alter the torque and rotational speed from the drive motor. In large, high-speed gear trains, fluid film bearings are often used. Fluid film bearings can be hydrostatic, hydrodynamic, or elastohydrodynamic [1]. This report considers gearboxes using hydrodynamic fluid film bearings. In hydrodynamic bearings, the load-carrying film is created and maintained by the shaft rotation. The design of the gear train affects the loads applied to the bearings in the system. The stiffness and damping characteristics of a fluid film bearing are drastically affected by the load magnitude and direction. Because of this, knowing the bearing loads inside a gearbox is crucial to the design of the system. The bearing loads are a result of the force vectors on the gear meshes. These force vectors create moments on the drive shafts that generate load vectors on each of the support bearings. Chapter 2 explains the derivation of equations necessary to find the load vector on a given bearing in a gearbox. A computer program written in Visual Basic.NET [2] is presented that calculates gearbox bearing loads bases upon user input of geometry, gear types, and input characteristics (i.e. rotational speed and power).

In high torque situations, it is desirable to use a split path gear train. A split path gear train divides the power into two separate paths and is the subject of Chapter 3. It is also sometimes referred to as a split torque gear train because the value of torque varies linearly with power. Split path gear trains designed with two separate gearboxes may also be called “back-to-back” arrangements. Many people who use split path gear trains do not fully understand them. Helicopter transmissions, ship

gearboxes, and high-speed test stands are some of the most common applications. In some split path gear trains the designer is concerned with ensuring that the power is split evenly between the parallel torque paths. This is the case in helicopter transmissions because the main purpose is to reduce the large loads on relatively small gears. In other situations, the designer intends to split the power unevenly. The uneven torque load has an effect on the bearing loads in the gearboxes. If there are fluid film bearings, a change in bearing load can have drastic effects in the stiffness. This report considers machinery intentionally designed with an uneven torque load.

The case study in this report is a test stand located at Wright Patterson Air Force base in Dayton, Ohio. The test stand is used for turbo machinery testing and is located in the Compressor Research Facility at the base. The test stand drive system consists of a large DC motor connected to two gearboxes in a “back-to-back” arrangement. Power is transmitted between the gearboxes by two quill shafts. Each quill shaft represents a different torque path. The gearboxes were designed during the 1960’s and there has not been much research into this type of split-path gearbox recently. Chapter 4 shows an analysis of the back-to-back gearbox arrangement at the CRF using the developed analytical model. The Visual Basic.NET computer program evaluates the specific design specifications of interest for the CRF test stand.

1.1 Literature Review

Much of the relevant research conducted on split path gear trains has focused on helicopter and marine gearboxes. Some of the findings from this research can be applied to all arrangements of split path gear trains.

Krantz [3] developed a method to analyze the load sharing of split path transmissions. Historically, planetary gear trains have been chosen for helicopter

transmissions. His objective was to demonstrate that split path gear trains, without additional load sharing devices, are an acceptable option for helicopter transmissions. The purpose of the analytical method that Krantz developed was to obtain an equal split of torque in the two power paths. He determined the machining tolerances that were necessary to have a torque split within specification.

Krantz, Rashidi, and Kish [4] compared the various methods for split torque load sharing. The goal was to have an even torque split in the two power paths. In split torque gear trains, load sharing devices aim to either; (1) accommodate deviations from ideal geometry to eliminate the no load backlash, or (2) minimize the torque required to bring the mesh with backlash into contact. The three methods of load sharing considered were (1) an epicyclic gear stage, (2) axial position of helical gears, and (3) compliance between the splitting mesh gears and the combining mesh pinions.

Rashidi [5] developed a mathematical model of a split torque gear train that includes a pivoting beam. The pivoting beam acts to balance thrust loads produced by the helical gear meshes in each of the two parallel power paths. When the thrust loads are balanced, the torque is split evenly. The effects of time varying gear mesh stiffness, static transmission errors, and flexible bearing supports are included in the model.

White [6] analyzed split torque gearboxes as a lightweight alternative to planetary gear trains in helicopters. Helicopter planetary gears, commonly employed at the reduction stage of the transmission, have reduction ratios no greater than 4.6:1. The required higher reduction ratio is obtained with stepped pinions that bring a major weight gain. White's alternative design adopts a double-helical gear at the output stage. The gear brings the ability to fit pinions of greater length than diameter which,

in combination with reduced tooth loading, allows a speed ratio about twice that of a simple planetary unit and concurrent reductions in gear weight and bearing weight.

1.2 Research Objectives

The major objective in this project is to analyze the bearing loads in a split path gear train. Knowing the bearing loads at various torque splits allows the calculation of the bearing stiffness and damping characteristics. The ability to calculate bearing characteristics under various loading conditions is crucial for troubleshooting machines that have a “back-to-back” gearbox arrangement.

The first step was to calculate the force vectors that helical and standard gear meshes create. These force vectors are used to determine the moments on the drive shafts which leads to the loads vectors on the bearings. The concepts of computing gear mesh forces are presented in Chapter 2. A Visual Basic.NET computer program is also introduced in Chapter 2 that calculates bearing loads in a single reduction gearbox. Chapter 3 goes a step further and explores the split path gear train. An analytical method is developed that computes the torque split at a given clocking angle and total input torque. The split path capability of the Visual Basic.NET program is shown in Chapter 3 as well. Chapter 4 presents a study of the Compressor Research Facility’s turbo machinery test stand located at Wright Patterson Air Force Base. The test stand data is entered into the analytical model as well as the Visual Basic.NET code. This information is currently being used to troubleshoot high vibration in the high-speed gearbox in the CRF drive system.

Chapter 2

Bearing Loads in a Gearbox

2.1 Introduction

In most industrial rotating equipment, the shaft loads the bearings in the direction of gravity. The shafts inside gearboxes have additional loading resulting from gear mesh forces. The loading becomes more complex when helical gears are used instead of spur gears. Helical gears have the benefit of transmitting heavier loads and higher speeds. This is due to the fact that spur gears generate more vibration. Any variation in a spur gear's involute profile will occur across the whole tooth face at the same time. This leads to a once-per-tooth excitation which can be very significant [7]. Helical gears can be applied for transformation of rotation between parallel or crossed axes. Involute helical gears with parallel axes are most common in gearboxes and will be considered in this report.

2.2 Concepts and Definitions

Helical gears that transform rotation between parallel axes in opposite directions are in external meshing and are provided with tooth screw surfaces of opposite direction. The direction of the tooth screw surface can be right-handed or left-handed. The tooth shape is referred to as an involute helicoid, which can be formed by unwrapping a parallelogram from a cylinder [8]. For meshing helical gears on parallel shafts, the helix angle is the same on both gears. The initial contact between helical gears occurs at a point. It increases to a line as teeth engage and more torque is applied. The contact line is a diagonal across the face of the tooth. Figure 2.1

illustrates the helical gear nomenclature. The symbol ψ represents the helix angle. As the helix angle approaches zero, the gear becomes a spur gear.

The helical gear terms are defined as:

$$p_t = \text{transverse circular pitch}$$

$$p_n = \text{normal circular pitch} = p_t \cos \psi$$

$$P_n = \text{normal diametral pitch}$$

The normal diametral pitch is related to the normal circular pitch by:

$$p_n P_n = \pi$$

$$P_t = \text{Transverse Diametral Pitch} = P_n \cos \psi$$

$$\phi_t = \text{transverse pressure angle}$$

$$\phi_n = \text{normal pressure angle}$$

It is important to note that $\phi_t \neq \phi_n$ unless the helix angle is zero. They are related by the equation:

$$\cos \psi = \frac{\tan \phi_n}{\tan \phi_t} \quad (2-1)$$

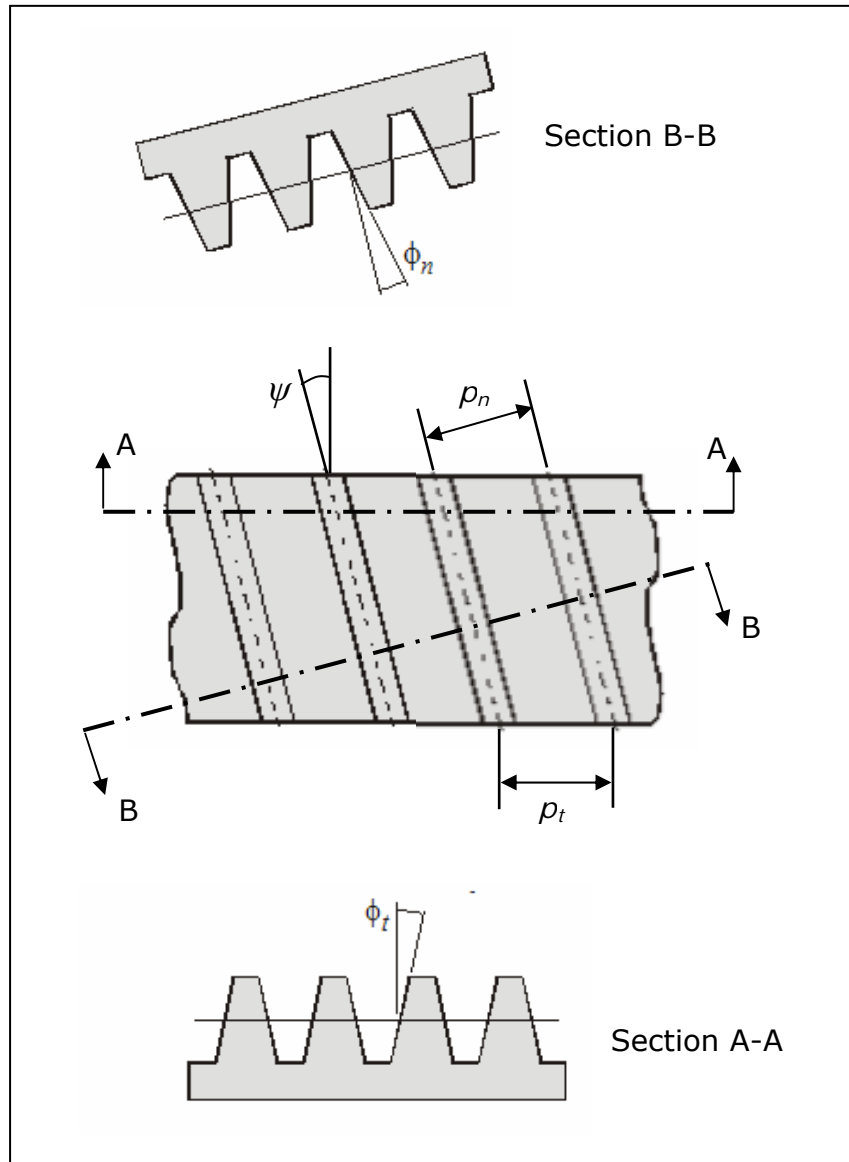


Figure 2.1
Helical Gear Nomenclature

In designing a gear, it is essential to analyze the magnitude and direction of the forces acting upon the gear teeth, shaft, bearings, etc. In analyzing these forces, an idealized assumption is made that the tooth forces are acting upon the central part of the tooth flank. Helical gears transmit axial and transverse loads. When the axial loads are too high or undesirable, two opposite helical gears mounted side by side are used. The

helical gear's transmission force, F_N , which is normal to the tooth surfaces, can be resolved into a tangential component, F_t , a radial component, F_r , and an axial component, F_a . The directions of these force components acting on a helical gear mesh are shown in Figure 2.2. The following equations define the three force components in terms of the resultant transmission force, F_n :

$$F_r = F_N \sin \phi_n \quad (2 - 2)$$

$$F_a = F_N \cos \phi_n \sin \psi \quad (2 - 3)$$

$$F_t = F_N \cos \phi_n \cos \psi \quad (2 - 4)$$

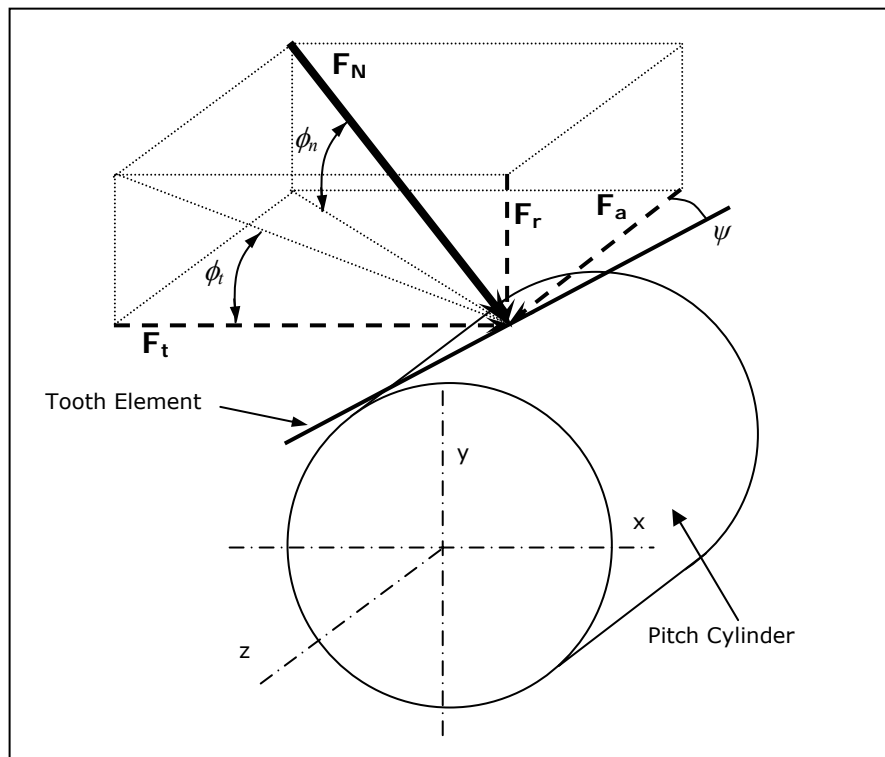


Figure 2.2
Helical Gear Mesh Force Components

The following equations express the force components in terms of the tangential forces, Equation 2-4:

$$F_r = F_t \frac{\tan \phi_n}{\cos \psi} = F_t \tan \phi_t \quad (2-5)$$

$$F_a = F_t \tan \psi \quad (2-6)$$

$$F_N = \frac{F_t}{\cos \phi_n \cos \psi} \quad (2-7)$$

The direction of the axial force varies depending on which helical gear is right-handed. Figure 2.3 shows the axial force directions for various combinations of helical gears. The axial thrust sub-component from the drive gear equals the driven gear's, but their directions are opposite. This rule also applies to the tangential components, F_t , and radial components, F_r .

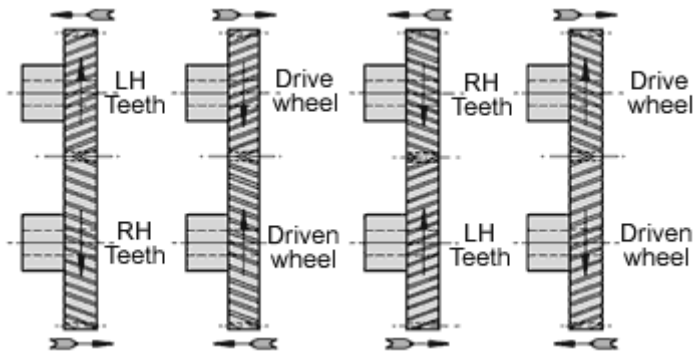


Figure 2.3
Helical Gear Axial Force Directions

2.3 Visual Basic.NET Code

The program that was developed, named *Gearbox Bearing Loads*, is capable of calculating the bearing loads in two different gear layouts. Visual Basic.NET is the programming language of choice for this project because it can generate a Microsoft Windows program that has an efficient Graphical User Interface (GUI). The two layouts are illustrated on the opening screen of the program in Figure 2.4. The “Gear Layout 1” option is discussed in this section. The “Gear Layout 2” option is explored in Chapter 3 when split path gear trains are discussed.

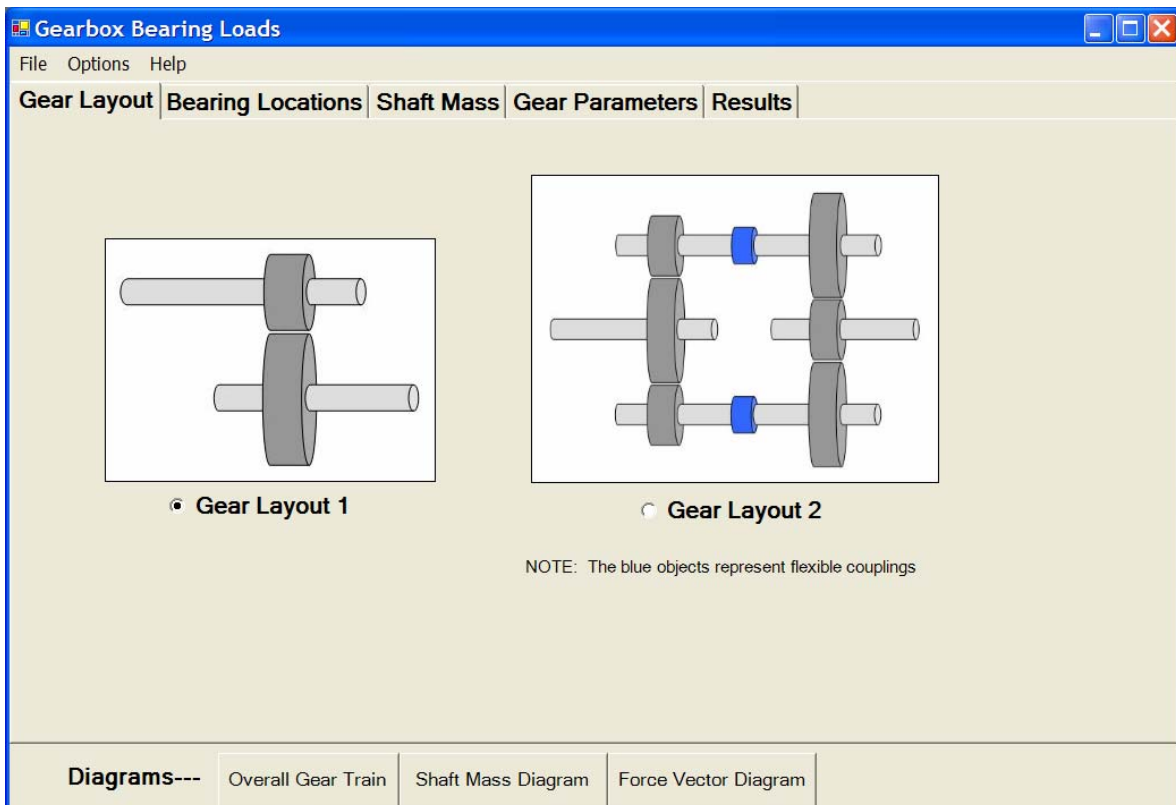


Figure 2.4
Gear Layout Option Screen
Gearbox Bearing Loads --Visual Basic.NET Program

The “Gear Layout 1” option represents a one-stage gear box with four bearings. The gears may be spur, single helical, or double helical. The various gear types are located in the “Options” menu located at the top of the program window. Figure 2.5 shows the “Force Vector Diagram” screen that defines the coordinate system and force vectors for each bearing. This diagram can be displayed at any time by clicking on the appropriate button on the bottom of the program window. The “Force Vector Diagram” also indicates the positive input shaft rotation direction.

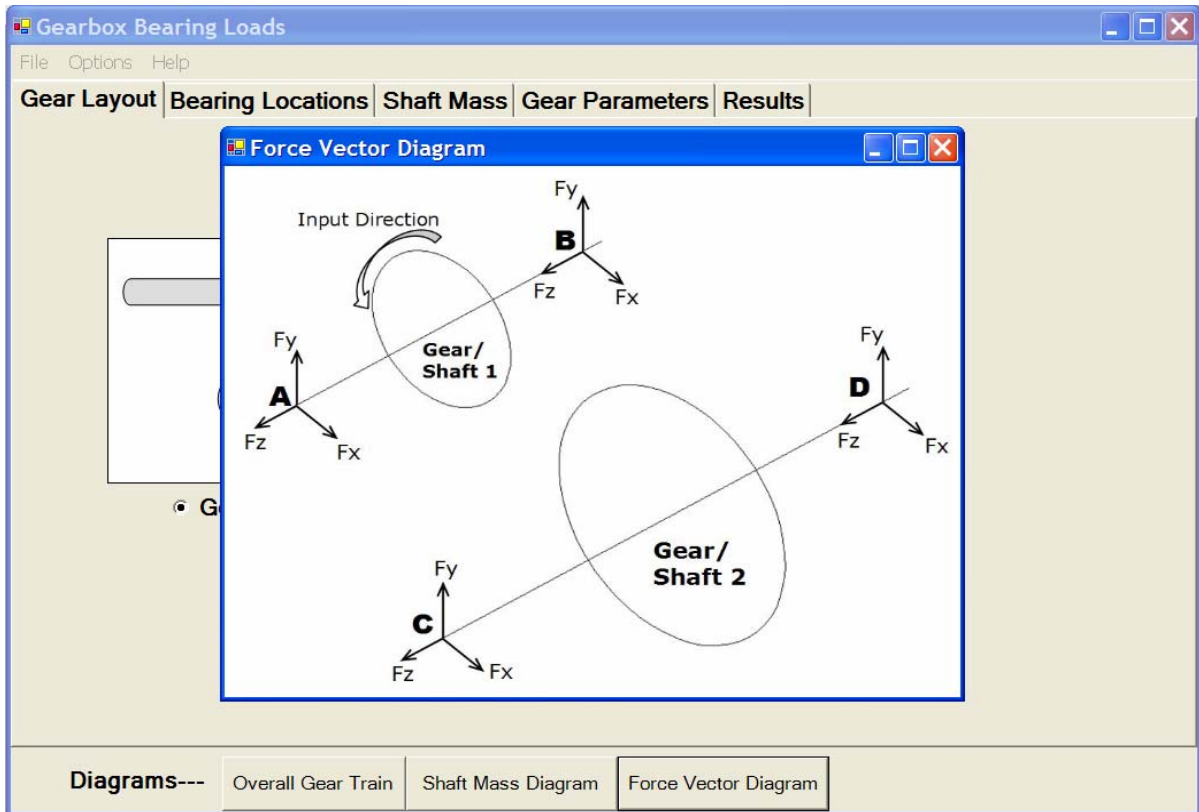


Figure 2.5
Force Vector Diagram for Gear Layout 1
Gearbox Bearing Loads --Visual Basic.NET Program

Figure 2.6 shows the screen where the user inputs the bearing locations. The inset picture is used as a guide for the bearing distance. It is possible to input a negative number for bearing distance if an overhung gear is desired. This same screen also allows the user to define the angle between the two meshing gears. The program is limited to a maximum angle “U” of 90 degrees and a minimum of 0 degrees.

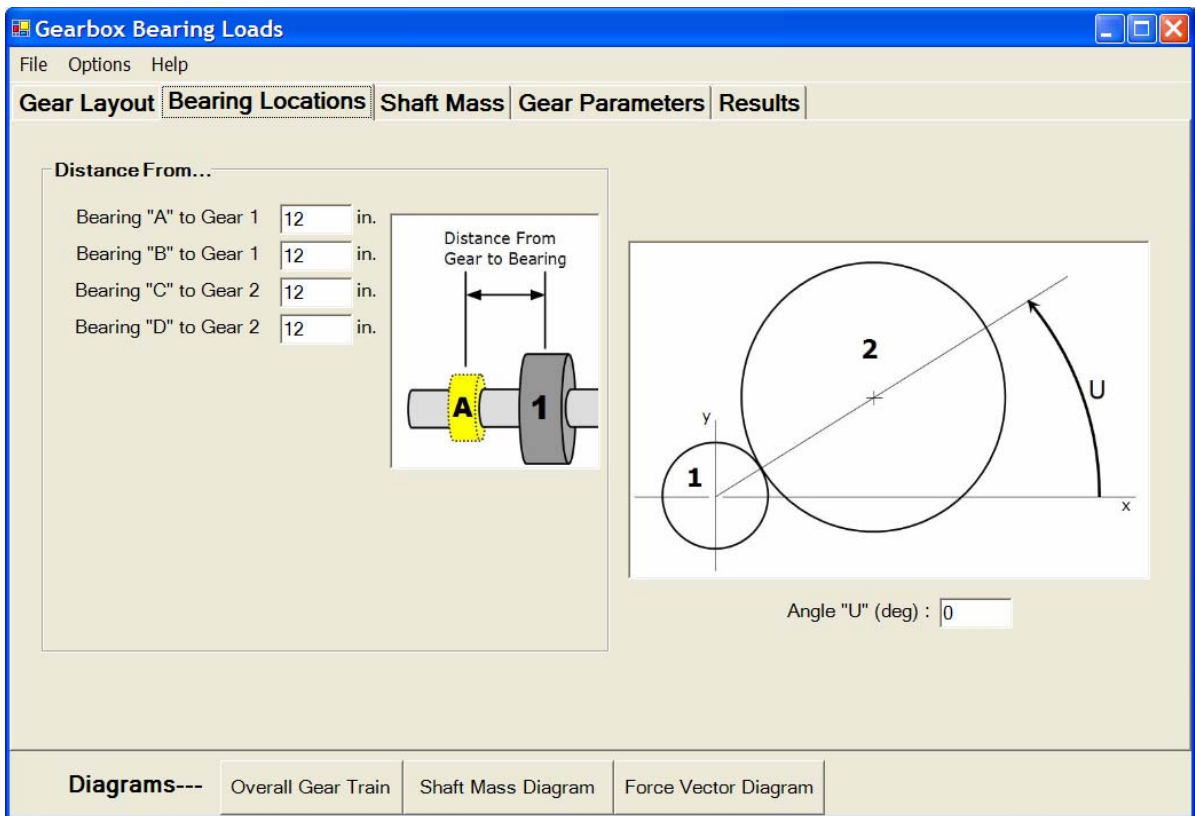


Figure 2.6
Bearing Location Input Screen for Gear Layout 1
Gearbox Bearing Loads --Visual Basic.NET Program

The shaft mass can be entered as lumped masses with designated locations. Figure 2.7 shows the input screen for the lumped masses as well as the “Shaft Mass Diagram” that defines the lumped mass distance from the bearings. The “Shaft Mass Diagram” can be displayed at any time by clicking on the appropriate button on the bottom of the program window. Negative values for the lumped mass distances are allowed.

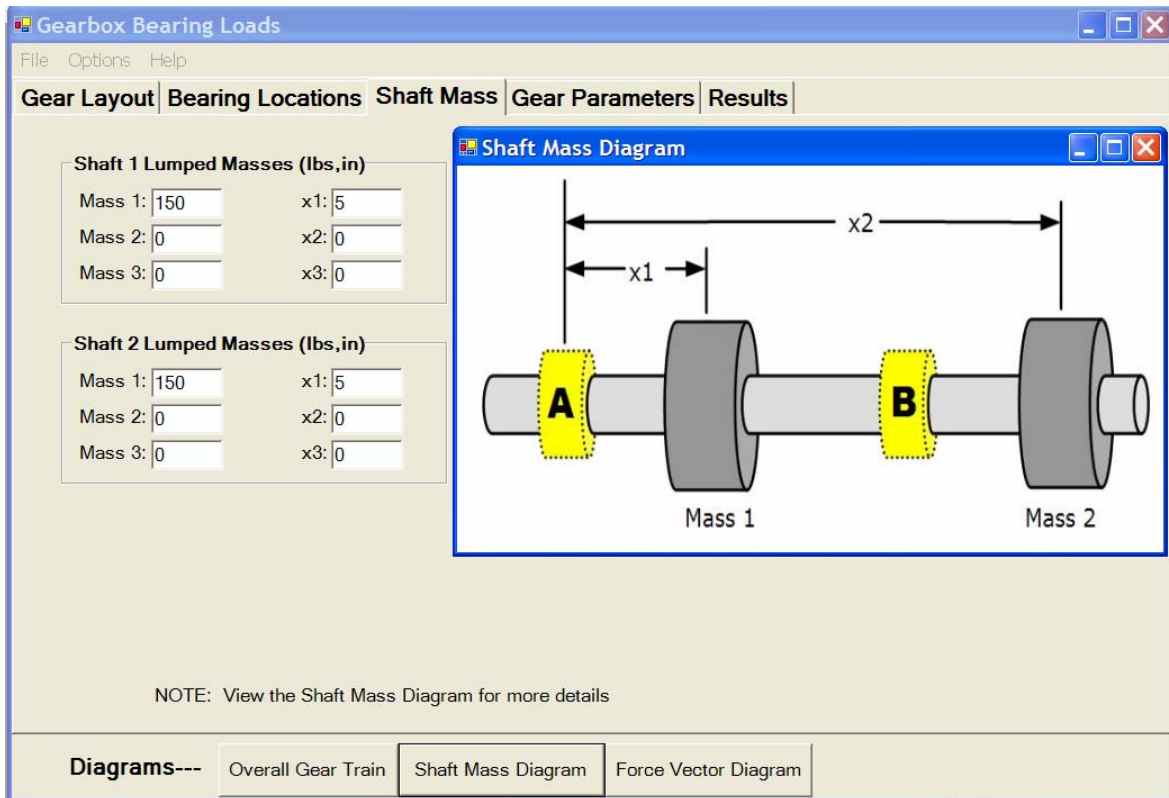


Figure 2.7
Shaft Mass Input Screen for Gear Layout 1
Gearbox Bearing Loads --Visual Basic.NET Program

The gear parameters are entered in the screen shown in Figure 2.8. The options on this screen vary depending on what options were chosen. For instance, if the spur gear type was chosen in the option menu, the helix direction drop-down menus would not be visible. The inset gear image can be used as reference for choosing the correct helix direction. If the “Metric” units menu option is chosen instead of the “Standard” units, the Diametral Pitch input switches to a Module input. Diametral Pitch (#teeth/in) and Module (mm) are inverses of one another.

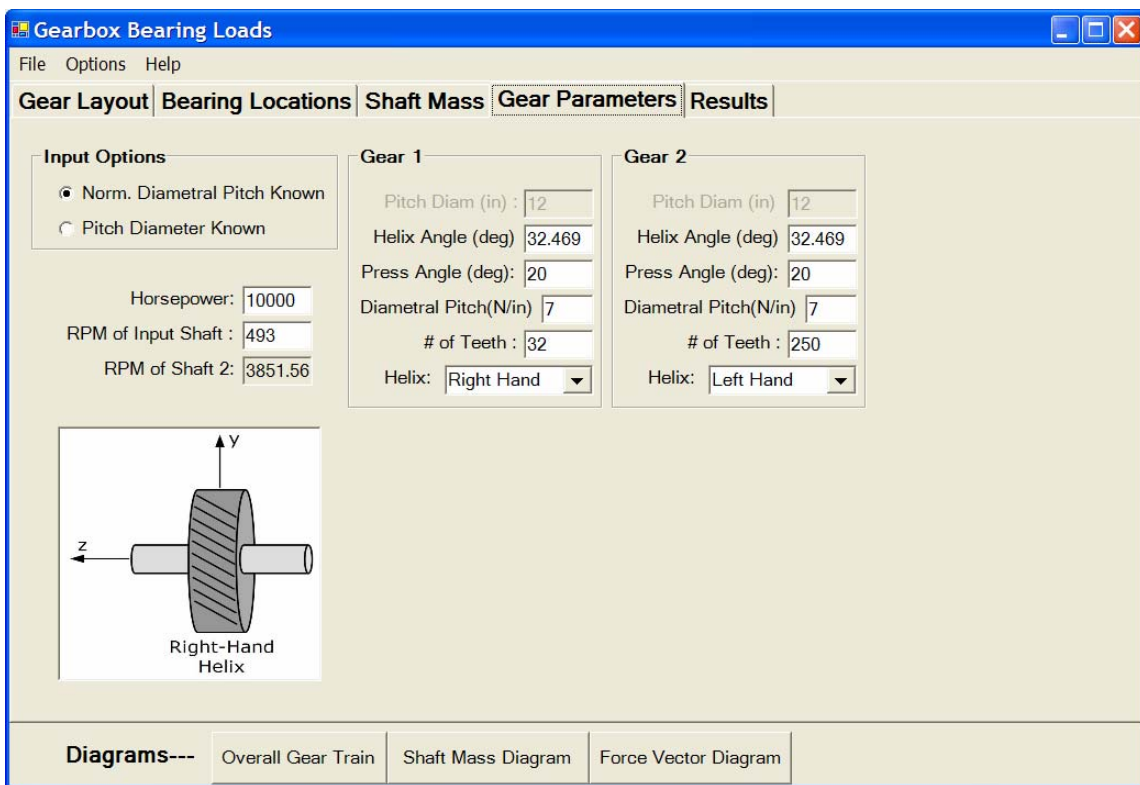


Figure 2.8
 Gear Parameter Input Screen for Gear Layout 1
 Gearbox Bearing Loads --Visual Basic.NET Program

When the “Results” tab is clicked, the Bearing Load subroutine is run and the results are displayed as shown in Figure 2.9. The Visual Basic.NET code for the subroutine is shown in Appendix A. The force analysis on the gear meshes uses the techniques described in the first section of this chapter. Equations 2-5 and 2-6 are used in the code to find the force components for each gear mesh. Moment calculations are used to find the resultant force on each of the four bearings. The shaft weights are calculated and displayed based on the lumped masses entered earlier. The “Force Vector Diagram” from Figure 2.5 can be displayed as reference when viewing the results screen.

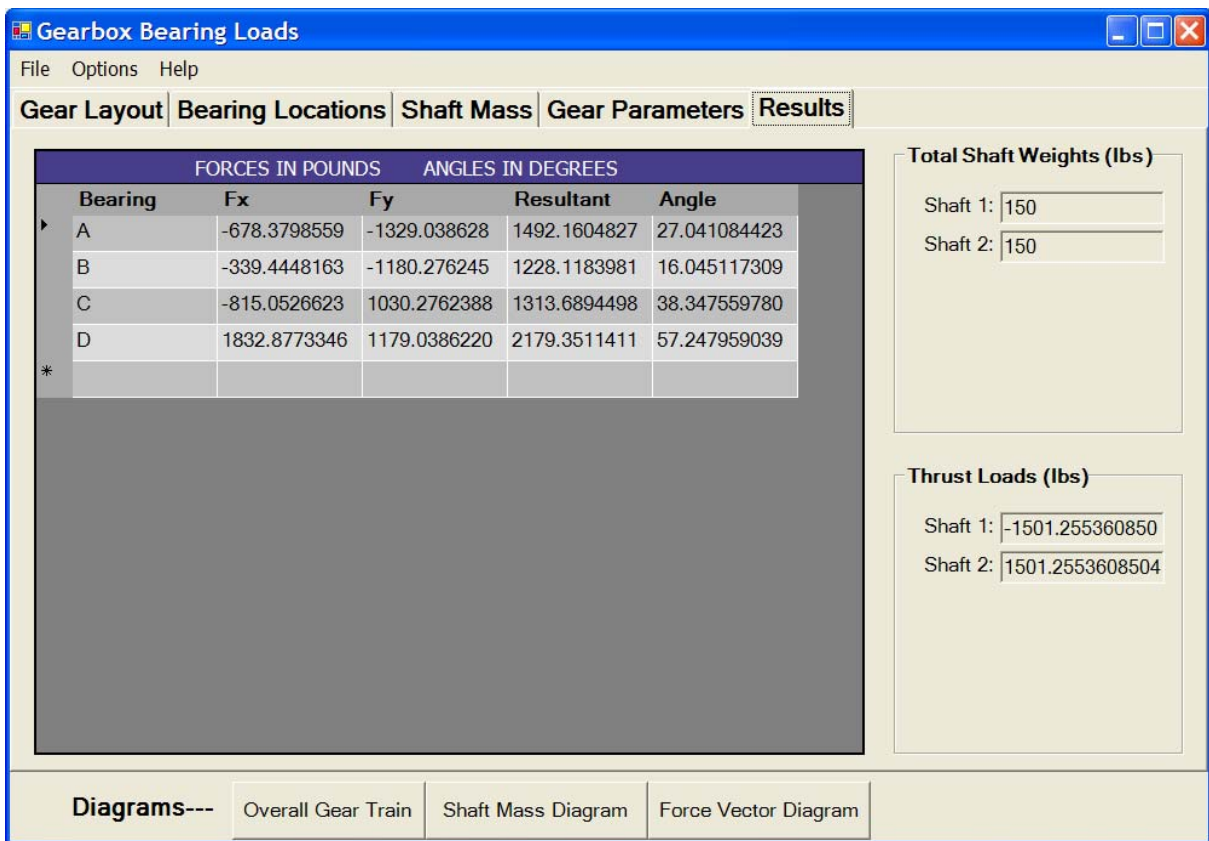


Figure 2.9
 Bearing Loads Result Screen for Gear Layout 1
 Gearbox Bearing Loads --Visual Basic.NET Program

Chapter 3

Split-path Gear Trains

3.1 Introduction

In this report, a split path refers to a parallel shaft gearing arrangement, such as shown in Figures 3.1 and 3.2, where the input pinion meshes with two gears, thereby offering two paths to transfer power to the output gear. This split path is usually built using two gearboxes in a “back-to-back” arrangement. But, for analytical analysis, it does not matter how many gearbox housings are present. The split path gear train has two speed reduction stages or two torque reduction stages.

3.2 Concepts and Definitions

In a gear mesh, the pinion is defined as the smaller of the two gears. The larger of the two gears is referred to as a bull gear. The following gear arrangement is for a split path gear train that increases speed and decreases torque. The input torque from the drive motor is applied to the initial bull gear. The bull gear of the first stage engages with two pinion gears. The power is split between these two pinions and carried by two second stage bull gears. The two bull gears drive the second stage pinion which is the output shaft. The design is similar to a planetary stage in that the torque is shared among multiple paths. To create the torque split, one of the power paths must have more torque than the other. This is achieved by leaving a predetermined gap between the gear teeth in one of the power paths. If a torque split of 0.50 is desired, and both power paths have the same stiffness, then all four gear meshes should be in contact with each other when there is no load in the system. In

order to create more torque in one path, three meshes will be in contact while the fourth mesh location will have some backlash. This can also be obtained by using a vernier gear coupling on one of the quill shafts.¹ As more torque is applied to the system, deformation will occur in the loaded path until the backlash at the fourth mesh location is eliminated. Since torque was absorbed in the quill shaft to eliminate the backlash, the load sharing will not be equal. The load sharing for this design will also be affected if the stiffness factors of the two load paths are not matched.

The two power paths are identified as A and B as shown in Figures 3.1 and 3.2. The clocking of a split path geartrain is an important attribute. For example, there are certain clockings where the geartrain could not be assembled because some of the gear teeth would interfere with one another. For this analytical section, the assembly of the gear mesh and the mating of the gear teeth are not considered. If the initial clocking angle gap is located in path A, then path B will initially carry more torque. Therefore, the initial clocking angle equals the effective angle in path B minus the effective angle in path A. Krantz [3] defined this effective angle as Loaded Windup. Equation 3-1 states the relationship between Loaded Windup in each path and the clocking angle, β . The gear ratio, GR, of the input bull gear to each of its meshing pinions is included in Equation 3-1 so that the torque values balance.

$$\beta = \frac{LWB - LWA}{GR} \quad (3-1)$$

$$LWA = \text{Loaded Windup in path A} = \frac{\tau_A}{k_A} \quad (3-2)$$

$$LWB = \text{Loaded Windup in path B} = \frac{\tau_B}{k_B} \quad (3-3)$$

¹ The vernier gear coupling arrangement is explained in more detail in chapter 4

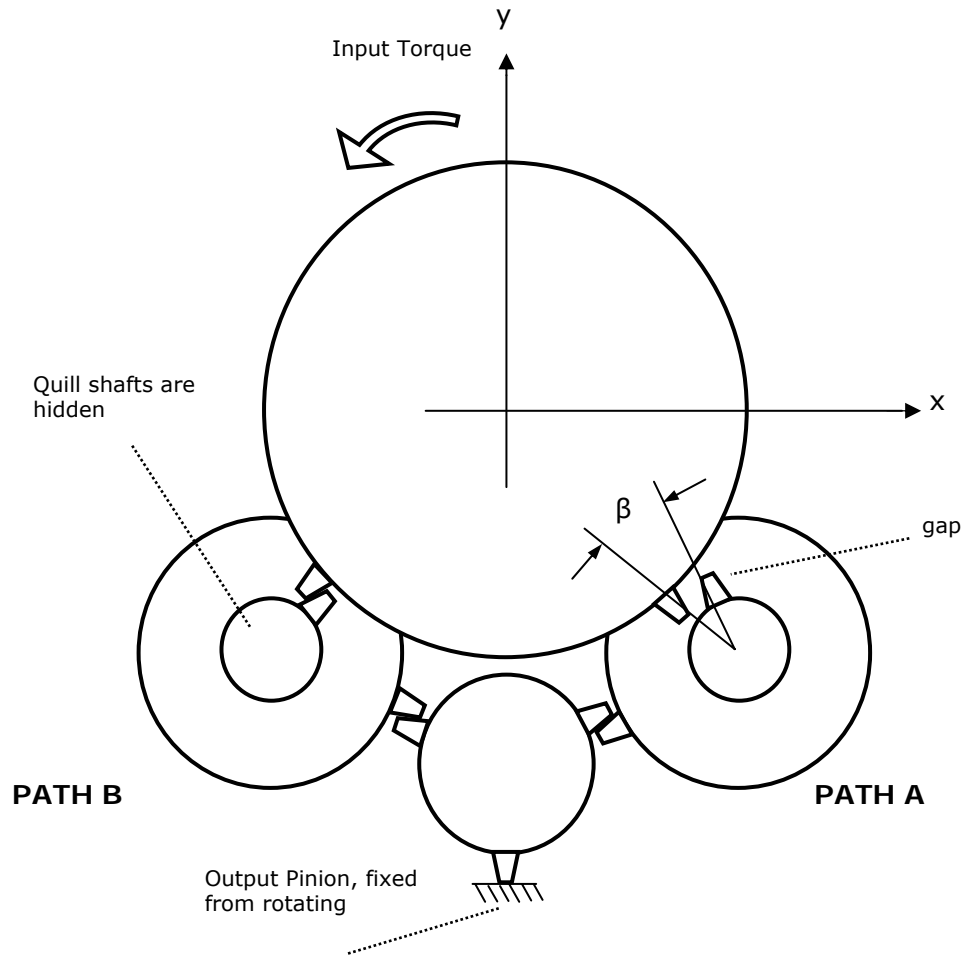


Figure 3.1
Split Path Gear Train -- Front View

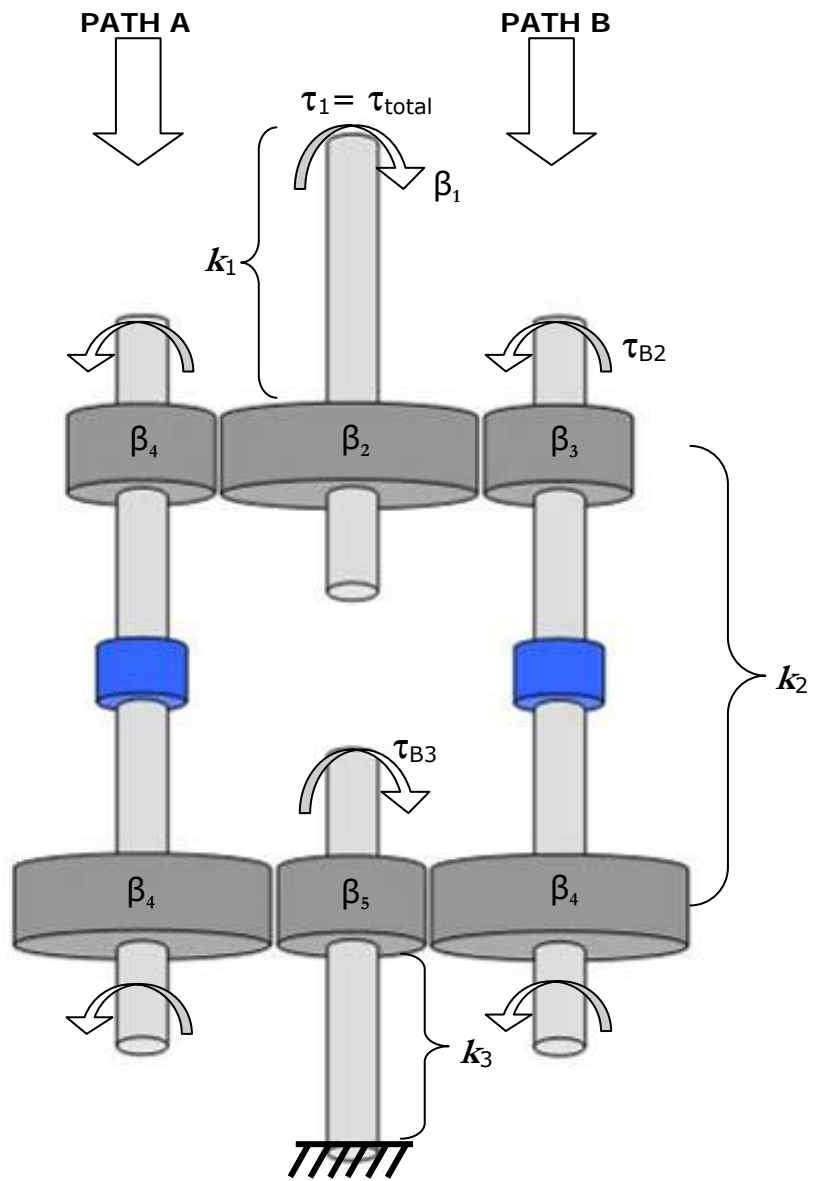


Figure 3.2
 Split Path Gear Train – Top View

Figure 3.3 shows a conceptual plot of the torque in each path as the input torque is increased. This plot represents a gear train that has paths of equal stiffness. The torque in path B will initially equal the input torque until all the gaps are closed. As the input torque is increased from this point, the gap will remain as the two lines remain parallel. The torque split in path B is the ratio of torque in path B over the total input torque. Although the torque lines have the same positive slope, the torque split is approaching 0.50 as the total input torque increase. This conceptual plot is verified in the next section. In addition, paths with different stiffness factors are considered.

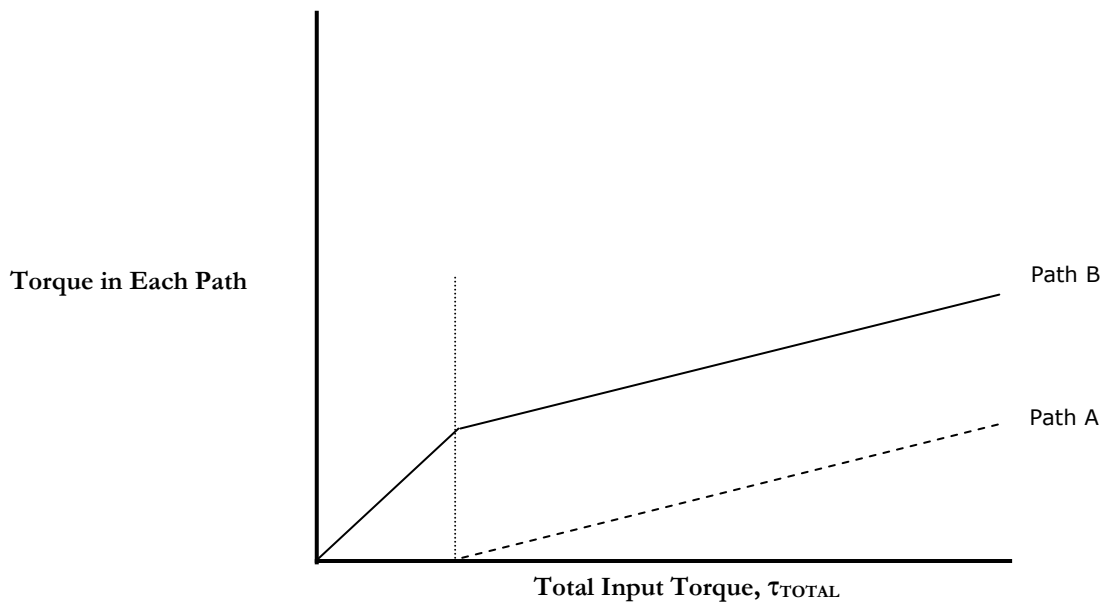


Figure 3.3
Conceptual Plot of Split Path Torque

3.3 Analytical Model

An analytical method was developed to study split-path load sharing. In so doing, the following assumptions were made:

- 1) The significant deformations that contribute to the loaded windups are quill shaft torsion and gear shaft torsion.
- (2) The effects due to gear tooth stiffness are insignificant compared to the quill shaft and gear shaft torsional stiffnesses.
- (3) Forces due to friction, thermal expansion, and inertia effects are negligible.

In this method the loaded windups of each load path are calculated for a given input torque and a given load split between the two power paths. The calculated loaded windups can then be used in Equation 3-1 to find the clocking angle β . The relationship between the clocking angle and load sharing can be established for a given input torque.

It was unclear whether or not the stiffness of shaft 1 and shaft 3 would affect the torque loading of the split path gear train. It is first necessary to state the relationships of the different torque and angle values using simple gear ratio operations:

$$\tau_1 = (GR_1)\tau_{B2} \quad (3-4)$$

$$\tau_{B2} = (GR_2)\tau_{B3} \quad (3-5)$$

$$\beta_2 = \left(\frac{1}{GR_1}\right)\beta_3 \quad (3-6)$$

$$\beta_4 = \left(\frac{1}{GR_2}\right)\beta_5 \quad (3-7)$$

Based on the definition of torque, the stiffness and torque equations are stated as:

$$\tau_1 = k_1(\beta_1 - \beta_2) \quad (3-8)$$

$$\tau_{B2} = k_2(\beta_3 - \beta_4) \quad (3-9)$$

$$\tau_{B3} = k_3\beta_5 \quad (3-10)$$

Substituting Equations 3-4, 3-5, 3-6, and 3-7:

$$\tau_1 = k_1(\beta_1 - \beta_2) \quad (3-11)$$

$$\frac{\tau_1}{GR_1} = k_2((GR_1)\beta_2 - \beta_4) \quad (3-12)$$

$$\frac{\tau_1}{GR_1} = k_3(GR_2)^2 \beta_4 \quad (3-13)$$

Rearranging Equation 3-13:

$$\beta_4 = \frac{\tau_1}{k_3(GR_2)^2 GR_1} \quad (3-14)$$

Rearranging Equation 3-12:

$$(GR_1)\beta_2 - \beta_4 = \frac{\tau_1}{k_2 GR_1} \quad (3-15)$$

Substituting Equation 3-14 into Equation 3-15 and rearranging:

$$\beta_2 = \frac{\tau_1}{k_2(GR_1)^2} + \frac{\tau_1}{k_3(GR_2)^2(GR_1)^2} \quad (3-16)$$

The satisfying condition for the clocking angle is:

$$\beta_2(\text{GR}_1) = \beta_{ini} + \beta_4 \quad (3-17)$$

Substituting Equations 3-16 and 3-14 into Equation 3-17 and rearranging:

$$\beta_{ini} = \frac{\tau_1}{k_2(\text{GR}_1)} + \frac{\tau_1}{k_3(\text{GR}_2)^2(\text{GR}_1)} - \frac{\tau_1}{k_3(\text{GR}_2)^2 \text{GR}_1} \quad (3-18)$$

The last two terms in Equation 3-18 cancel each other leaving:

$$\beta_{ini} = \frac{\tau_1}{k_2(\text{GR}_1)} \quad (3-19)$$

It is clear that the stiffness factors of shaft 1 and shaft 3 do not have an effect on the torque loading of the gear train. Equation 3-19 is not a function of k_1 , k_3 , or GR_2 . This means that it is irrelevant whether the load is held fixed or the secondary bull gear is held fixed. This proof also indicates that Equation 3-1 will apply to all split path gear trains.

Using Krantz's expression for the clocking angle the torque in each path is derived. Substituting Equations 3-2 and 3-3 into equation 3-1:

$$\beta(\text{GR}) = \frac{\tau_B}{k_B} - \frac{\tau_A}{k_A} \quad (3-20)$$

By definition:

$$\tau_A = \tau_{total} - \tau_B \quad (3-21)$$

The torque in path A can be expressed in terms of the total input torque and the torque in path B by substituting Equation 3-21 into Equation 3-20 and rearranging:

$$\frac{\tau_B}{k_B} = \frac{(\tau_{total} - \tau_B)}{k_A} + \beta(\text{GR}) \quad (3-22)$$

Rearranging Equation 3-22 results in the expression for torque in path B:

$$\tau_B = \frac{k_B \tau_{total}}{(k_A + k_B)} + \frac{k_A k_B \beta(\text{GR})}{(k_A + k_B)} \quad (3 - 23)$$

If the stiffness factors of each path are the same, then the equation for torque in path B simplifies to:

$$\tau_B = \frac{\tau_{total}}{2} + \frac{\beta(\text{GR})k_B}{2} \quad (3 - 24)$$

Using the same derivation as Equation 3-23, the torque in path A is found:

$$\begin{aligned} \frac{(\tau_{total} - \tau_A)}{k_B} - \frac{\tau_A}{k_A} &= \beta(\text{GR}) \\ \tau_A \left(\frac{k_B + k_A}{k_B k_A} \right) &= \frac{\tau_{total}}{k_B} - \beta(\text{GR}) \\ \tau_A &= \frac{k_A \tau_{total}}{(k_A + k_B)} - \frac{k_B k_A \beta(\text{GR})}{(k_A + k_B)} \end{aligned} \quad (3 - 25)$$

Next, the equation for the torque split in path B is derived. The definition of torque split is:

$$\text{Torque Split}_B = \frac{\tau_B}{\tau_{total}} \quad (3 - 26)$$

Substitution Equation 3-23 into Equation 3-26:

$$\text{Torque Split}_B = \frac{k_B}{(k_A + k_B)} + \frac{k_A k_B \beta(\text{GR})}{\tau_{total} (k_A + k_B)} \quad (3 - 27)$$

The plot shown in Figure 3.4 was generated using Equation 3-24. This plot shows how each path carries the torque when the stiffness factors in each path are equal. The plots shown in Figures 3.5 and 3.6 were generated using Equation 3-23. Arbitrary values of β , GR, and stiffness factors were used so that the torque splitting effect could be visualized. The plot in Figure 3.5 represents the torque in each path when path B has a higher value of stiffness. Initially, path B takes all the torque. Once the clocking angle gap is closed in path A, path B continues to carry more of the torque because it has a higher stiffness factor. Figure 3.6 shows the torque relationship when path A has a higher stiffness factor. Again, path B takes all the input torque until the clocking angle gap is closed in path A. The difference is that the slope of path A is greater than the slope of path B due to the higher stiffness in path A. At a certain input torque, the torque in path A will surpass the torque in path B and continue increasing the gap. Having the ability to plot the torque relationship between paths for given geometry will help designers choose the appropriate torque split. If an equal torque split is desired, the same equations can be used to find the desired clocking angle.

Torque in Each Path as a function of Total Input Torque

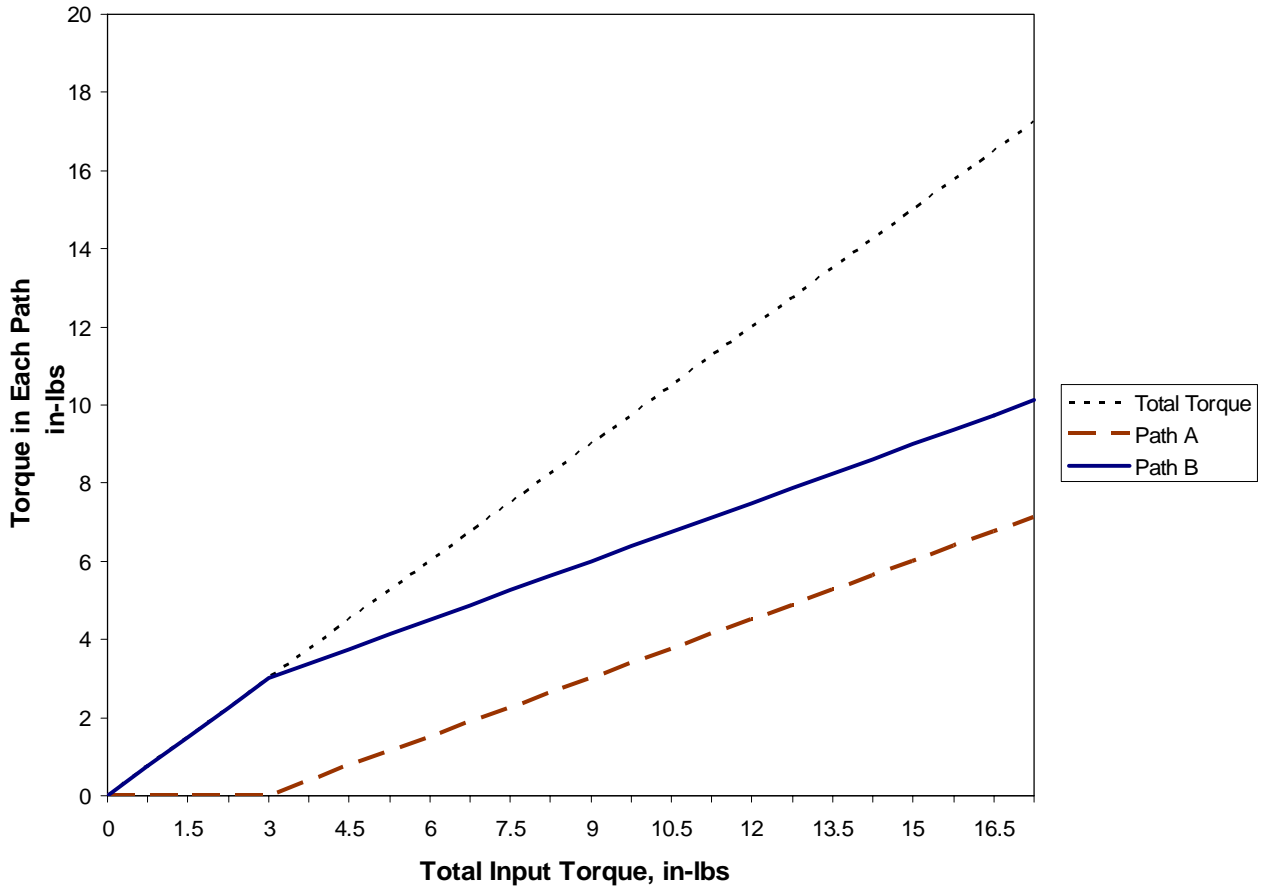


Figure 3.4

Split Path Torque -- Each torque path has identical stiffness

$\beta = 0.02$ radians , GR = 5

$K_A = 30$ in-lbs/rad , $K_B = 30$ in-lbs/rad

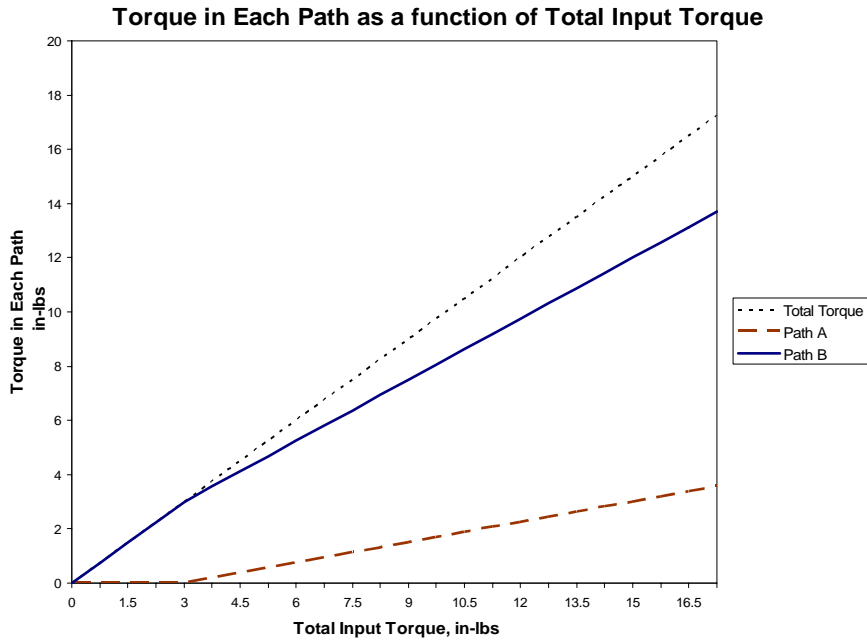


Figure 3.5
 Split Path Torque -- Torque path B has greater stiffness than path A
 $\beta = 0.02$ radians , $GR = 5$
 $K_A = 10$ in-lbs/rad , $K_B = 30$ in-lbs/rad

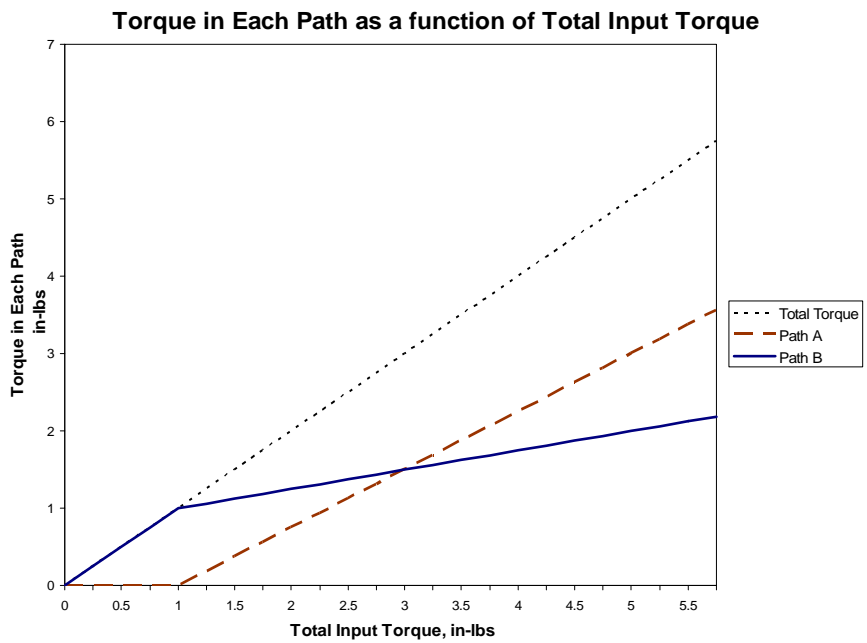


Figure 3.6
 Split Path Torque -- Torque path A has greater stiffness than path B
 $\beta = 0.02$ radians , $GR = 5$
 $K_A = 30$ in-lbs/rad , $K_B = 10$ in-lbs/rad

3.4 Computer Program Split Path Calculation

The *Gearbox Bearing Loads* computer program is capable of analyzing the bearing loads in split path gear trains. Recalling from Chapter 2, the “Gear Layout 2” option on the initial screen represents the split path gear train. It uses the same gear tooth force algorithm that is used in the “Gear Layout 1” choice. In addition, the split torque concepts described in this chapter are applied. Figure 3.7 shows the bearing and gear arrangement used for “Gear Layout 2”. If the torque was evenly split (Torque Split = 0.50), then gears 2 and 5 would be completely unloaded. The forces introduced from their mating gears would cancel out. The “Gear Layout 2” algorithm handles twelve bearings instead of four. A segment of the Visual Basic.NET code is located in Appendix B.

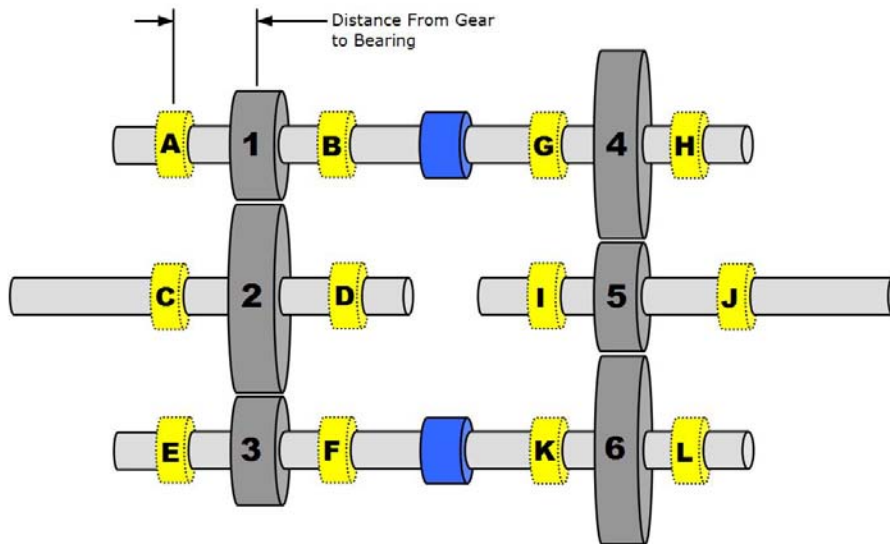


Figure 3.7
Bearing and Gear Arrangement for Gear Layout 2

The two force vector diagrams for “Gear Layout 2” are shown in Figure 3.8. These diagrams define the force vector directions for each of the twelve bearings as well as the input rotation direction. These two diagrams can be displayed at any time by clicking on the appropriate buttons on the bottom of the program window. The “Force Vector Diagram” also indicates the positive input shaft rotation direction.

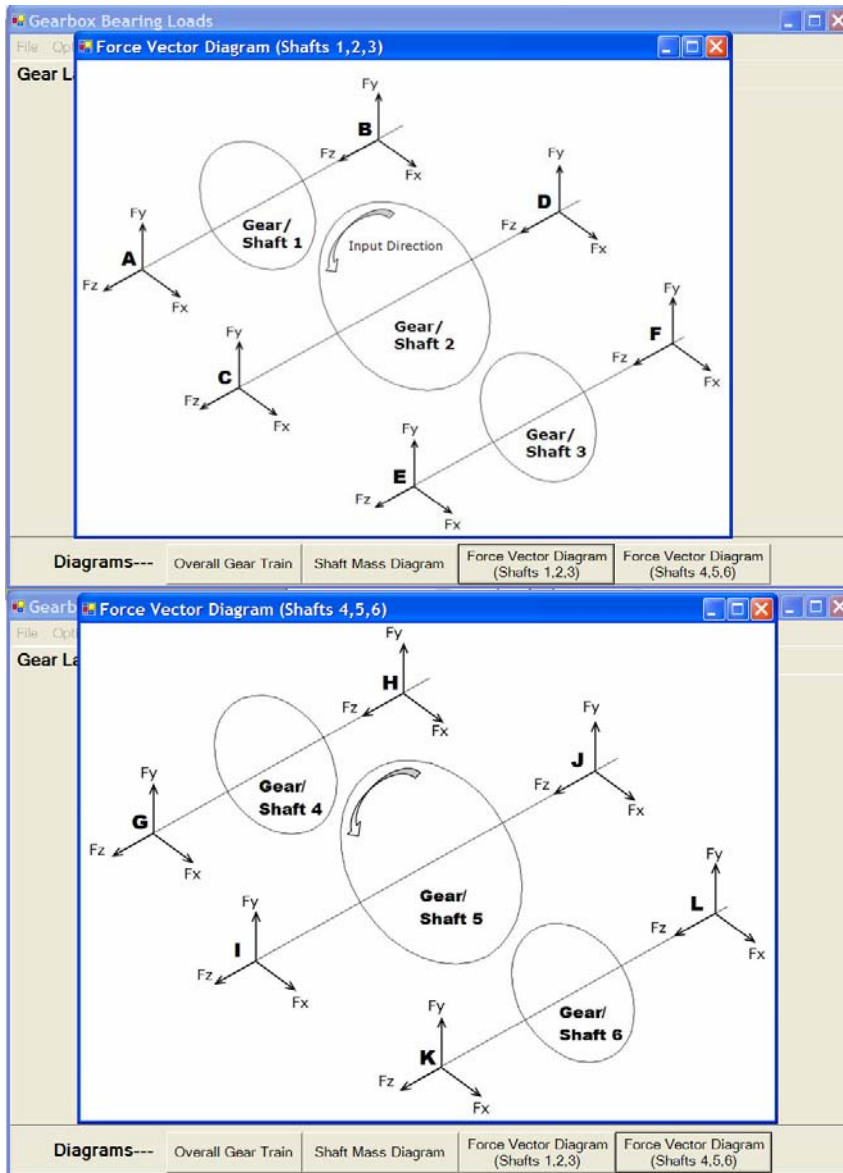


Figure 3.8
Force Vector Diagrams for Gear Layout 2
Gearbox Bearing Loads Visual Basic.NET Program

The bearing locations are entered in the screen shown in Figure 3.9. There are twelve inputs instead of the four inputs for the “Gear Layout 1” option. The inset picture is used as a guide for the bearing distance. It is possible to input a negative number for bearing distance if an overhung gear is desired. This same screen also allows the user to define the angle between the two meshing gears. There is an additional shaft position angle input for the second gearbox. The angles “U” and “V” are limited to a maximum of 90 degrees and a minimum of 0 degrees.

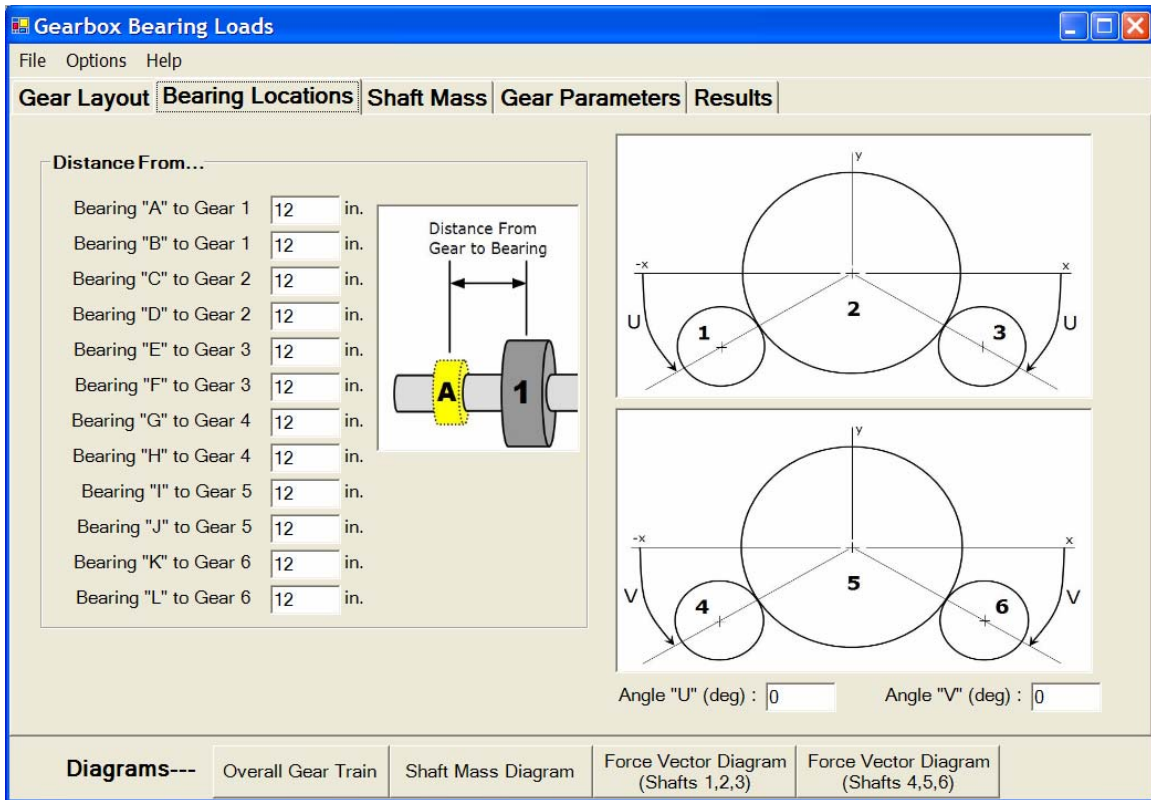


Figure 3.9
 Bearing Location Input Screen for Gear Layout 2
 Gearbox Bearing Loads Visual Basic.NET Program

The gear parameters are entered into the screen shown in Figure 3.10. This split path layout has additions to the gear parameter screen in “Gear Layout 1”. One difference is the torque split that is entered into this screen. The value of torque split is calculated using the analytical model derived in section 3.5 of this chapter. Another addition is the ability to enter parameters for six gears instead of two.

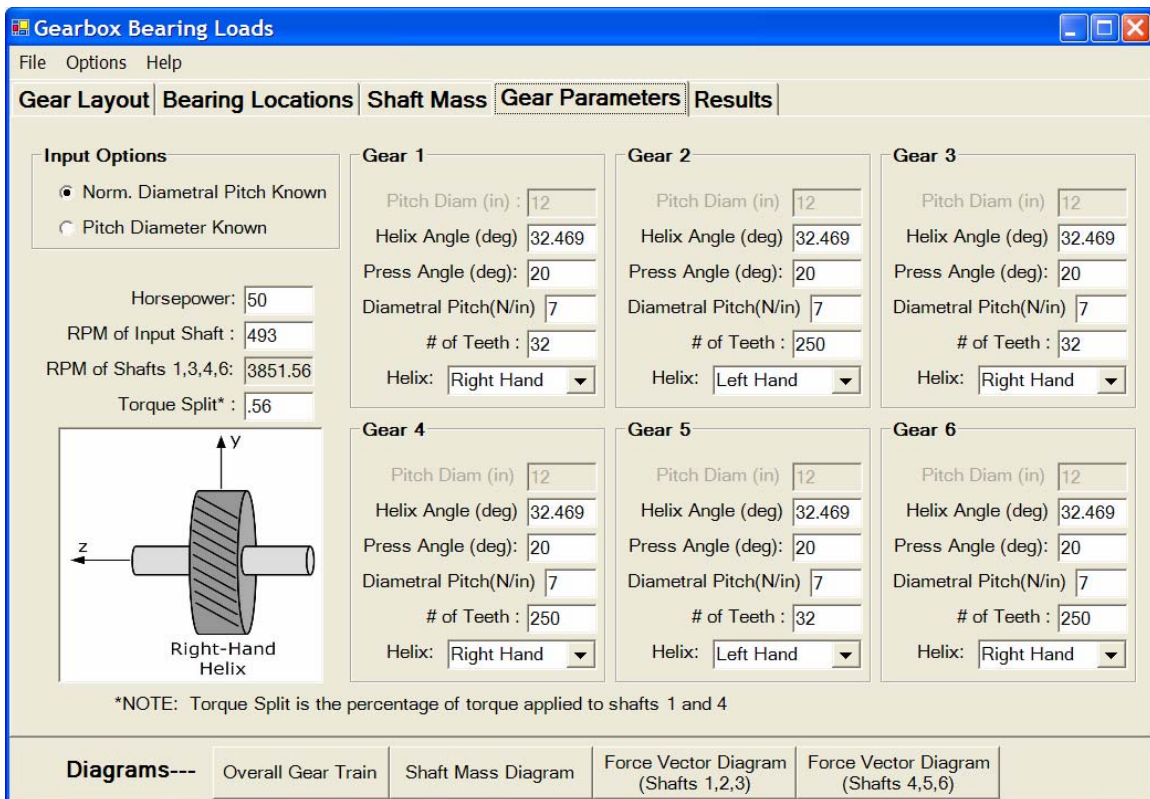


Figure 3.10
Gear Parameter Input Screen for Gear Layout 2
Gearbox Bearing Loads Visual Basic.NET Program

When the “Results” tab is clicked, the Bearing Load subroutine is run and the results are displayed as shown in Figure 3.11. A segment of the Visual Basic.NET code for the subroutine is shown in Appendix B. The value of Torque Split entered in the “Gear Parameter” screen is used to calculate the percentage of total torque in each path. The force analysis on the gear meshes uses the techniques described in chapter 2. Equations 2-5 and 2-6 are used in the code to find the force components for each gear mesh. Moment calculations are used to find the resultant force on each of the four bearings. The shaft weights are calculated and displayed based on the lumped masses entered earlier. The “Force Vector Diagrams” from Figure 3.8 can be displayed as reference when viewing the results screen.

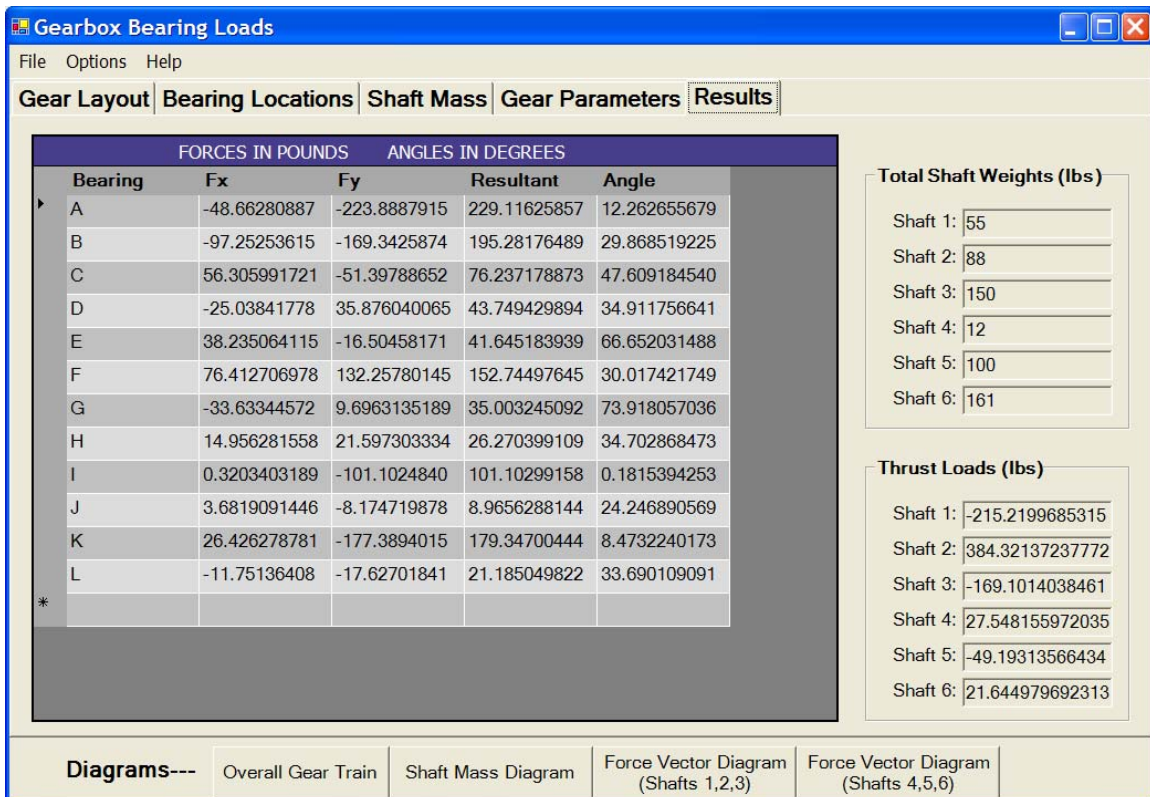


Figure 3.11
Bearing Loads Result Screen for Gear Layout 2
Gearbox Bearing Loads Visual Basic.NET Program

Chapter 4

Case Study: CRF Test Stand

4.1 Introduction

The inspiration for this report is a turbo machinery test stand located in the Compressor Research Facility (CRF) at Wright Patterson Air Force base in Dayton, Ohio. The test stand consists of two large DC motors connected to two gearboxes in a “back-to-back” arrangement. Power is transmitted between the gearboxes by two quill shafts. The gear train arrangement is shown in Figure 4.1. Each quill shaft represents a different torque path. The gearboxes were designed during the 1960's and there has not been much research into this type of split-path gearbox recently. The CRF test stand has never achieved its design speed of 30,000 RPM according to information supplied by the engineers involved with the operation. One of the gearboxes operated at the CRF is thought to be one of the sources of the difficulty. This gearbox, known as High Speed Gear Box III (HSGB III), was received in the 1970's from Philadelphia Gear Corporation. It has seldom been run at speeds above 24,000 RPM because of excessive motion at the journal bearings that support the shafts and gears. Preliminary data acquired in 1998 by Air Force personnel indicated that the problems with HSGB III might have been related to resonances in the gearbox.

A former work performed by the University of Dayton Research Institute (UDRI) was to augment the data measured by the Air Force and to determine what changes might be required to enable the gearbox to achieve its design speed. The overall conclusion of that work (Sept., 1999) was namely that the problem was thought to be a resonance in the drive system quill shafts and that by stiffening one key

component, the resonance frequency would move outside the operating speed range. The implementation of that fix was made and the information provided was that it did not solve the problem.

Additional data has been taken by WPAFB in August 2001 and more extensive data reported by Bently Nevada in a report dated 28 November 2001. These reports indicate a possible resonance or other source of excessive vibration above 16,000 rpm for the reverse direction operation of HSGB III. Variations of torque split in the two drive shafts were also made with some improvement but other related problems. A change of the high speed pinion bearing design was one recommendation made in that report. No analysis was provided to support the recommendation.

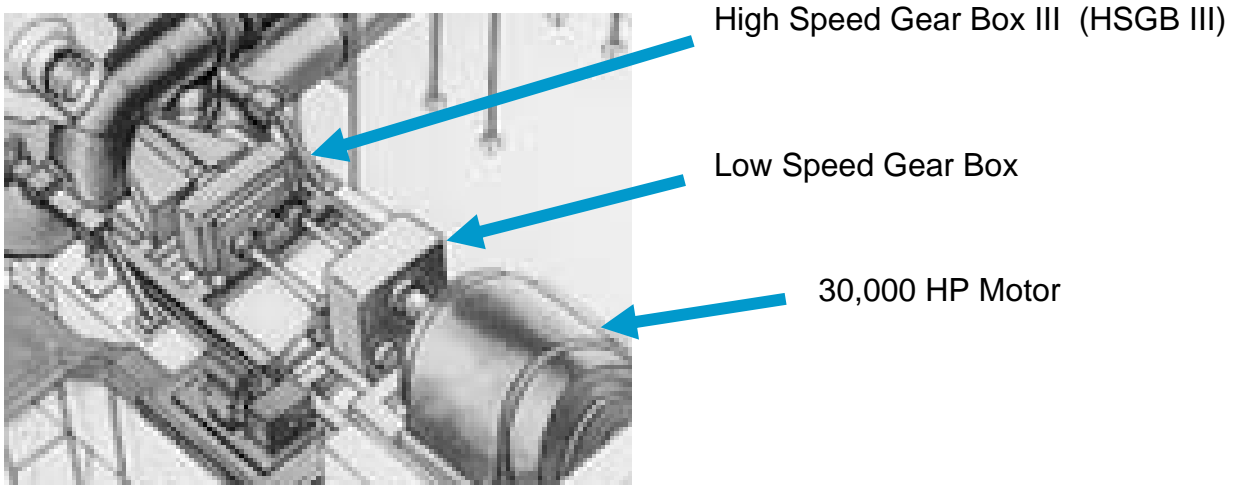


Figure 4.1
CRF Test Stand Gear Train

Once the CRF vibration problem was introduced to Virginia Tech, the first goal was to verify that the models of the system were consistent. The High Speed Pinion was modeled in two separate rotor dynamics analysis programs. DyRoBeS [9] uses a

finite element code to solve the system. VT-FAST [10] uses a code that solves the system incrementally along the shaft. Table 4.1 shows a sample of the results from the two different programs. The results from DyRoBeS and VT-FAST were consistent with each other so either program could be used in confidence. The preference was to use DyRoBeS and its companion program BePerf [11] (used for bearing analysis). All the shafts in the CRF drive train were subsequently analyzed in DyRoBeS.

TABLE 4.1 -- Comparison Between DyRoBeS and VT-FAST Software

	log dec	Damped Natural Freq (rpm)	Whirl Direction
DyRoBeS	0.55	16,372	Stable Forward
VT-FAST	0.5468	16,304	Stable Forward
% difference	-0.58 %	-.041 %	--

NOTE: % difference is defined as
 $(\text{DyRoBeS} - \text{VT-FAST}) / \text{VT-FAST} \times 100$

The DyRoBeS model of the High Speed Pinion is shown in Figure 4.2. The bearings are estimated for the initial model because the bearing profile was unknown. At this point the bearings were only known to be 4 lobed. The drive coupling that connects the H.S. Pinion to the output shaft (jackshaft) is modeled as lumped masses. The masses are shown as circles on the right side of the model in Figure 4.2. The loading applied to the bearings caused by the torque split was not calculated. This simplified model gave useful initial results of the critical speeds, forced response to unbalance, and stability.

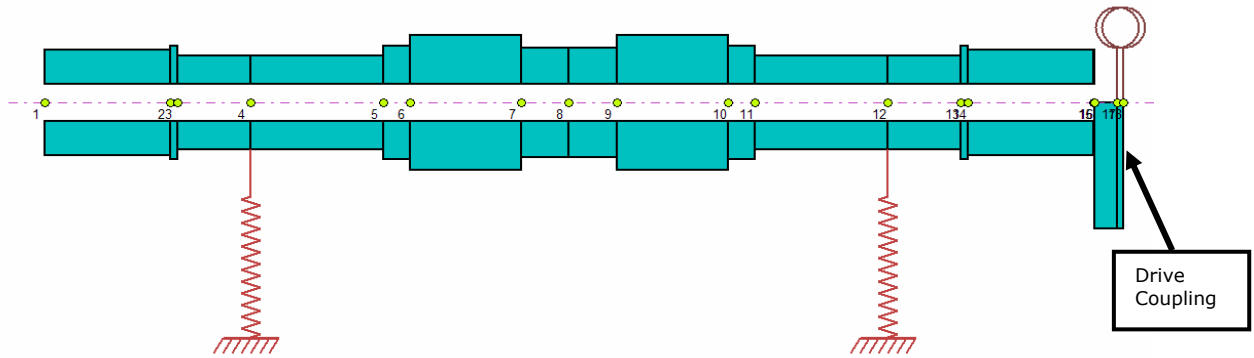


Figure 4.2
High Speed Pinion Shaft DyRoBeS Model
with jackshaft coupling weight

Figure 4.3 shows the forced response at various locations along the High Speed Pinion. This model uses estimates for the bearing profiles and loading. There appears to be a critical speed located between 28,000 – 30,000 rpm. The unbalance was placed at the coupling end and that explains the high magnitude of response on that end.

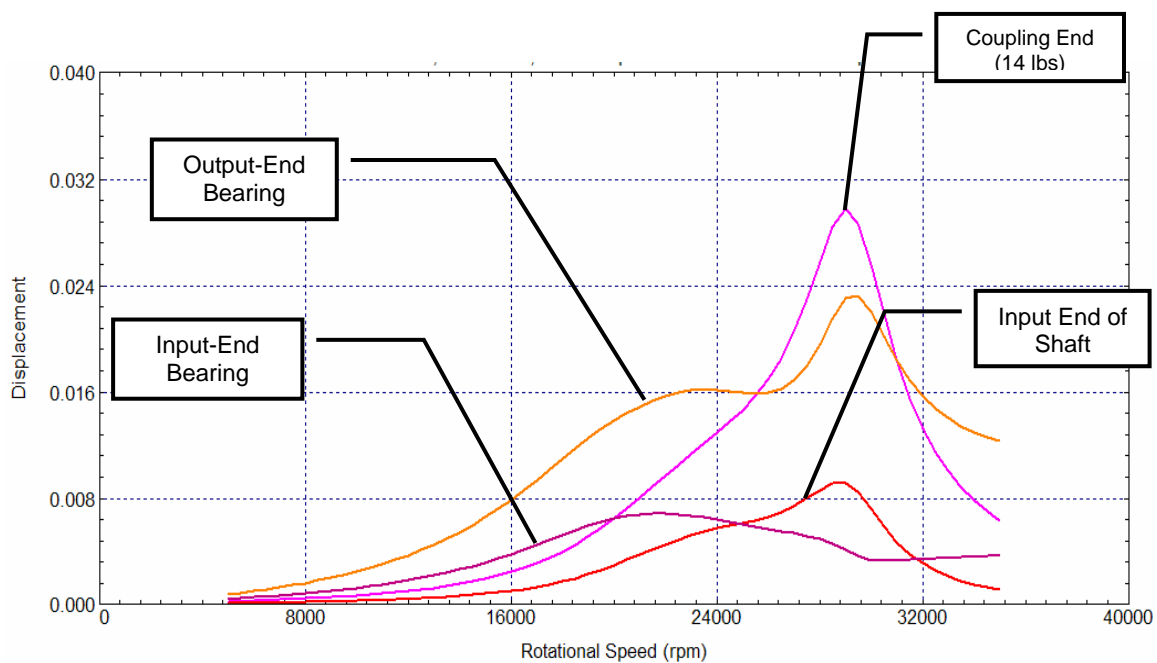


Figure 4.3
Multiple Station Forced Response with
estimated bearing loading

One of the improvements to the model was to obtain an accurate bearing profile for the High Speed Pinion bearings and the bull gear/shaft bearings. Once Virginia Tech had possession of the bearings, the profiles could be accurately measured. An inside micrometer was used to measure the inside diameter of each bearing at 6 positions around the circumference. At each position there was an identifiable mark or characteristic so that the measurements could be repeated. This method was successful for measuring the bull gear/shaft bearing since the profile was cylindrical. The inner diameter is constant at 6.2583 inches. In addition, there are two pockets that are 20 degrees each. The pocket depth is 0.185 inches.

The initial measurements taken on the HS pinion shaft bearing were not detailed enough to be used for analysis. The HS Pinion bearing is a four-lobe bearing so the profile is more complicated. A protractor was used to mark off 5 degree increments all the way around the bearing. Diameter measurements were taken at every mark. This resulted in four segments that should theoretically be the same. This made it easier to check the repeatability of the readings. The data was entered into excel and created a bearing profile “chart”. The bearing profile is shown in Figure 4.4. The measured data looks smoother in over some lobes than others. In this case the smoothest data was chosen, and the jagged measurements were discarded. There are four pockets that are 20 degrees each. The pocket depth is roughly 0.19 inches.

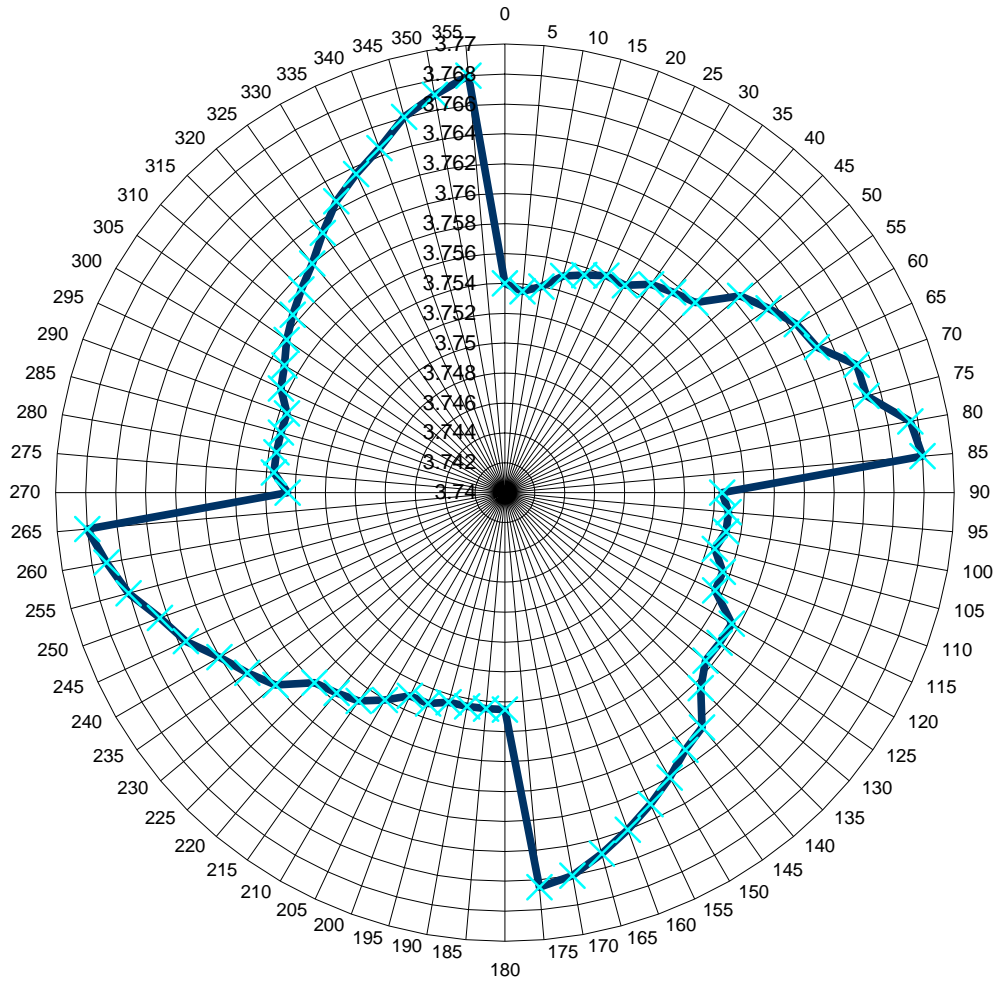


Figure 4.4
High Speed Pinion Shaft Bearing Profile

Although the bearing profile was mapped out, the parameters to enter into BePerf (the bearing analysis program) were still needed. BePerf has inputs such as preload, offset, and radial bearing clearance. BePerf uses an analytical profile curve when calculating bearing characteristics. This analytical profile curve of a 4-lobe bearing is thought to be well defined as an equation in the rotor dynamics industry. The film thickness is expressed as a function of the pad clearance by:

$$h(\theta) = C_p - r_p \cos(\theta_L + \alpha\chi - \theta) - x \cos \theta - y \sin \theta \quad (4 - 1)$$

where :

C_p = Lobe radial clearance

$r_p = \delta * C_p$

δ = preload

θ_L = angle to leading edge

α = offset

χ = angular extent of lobe

Preload is an internal loading characteristic in a bearing which is independent of any external radial and/or axial load carried by the bearing. It is a dimensionless quantity that is typically expressed as a number from zero to one where a preload of zero indicates no bearing load upon the shaft, and one indicates the maximum preload (i.e., line contact between shaft and bearing).

A MATLAB [12] program was created that would plot the measured bearing profile data points on top of the analytical profile curve. The program gave us the ability to change the offset and preload values of the analytical curve until it matched the measured bearing profile. Figure 4.5 shows the final Matlab plot. The red circle represents the shaft. The shaft radius is set to 10 mils so that the bearing profile curves could be relatively large and easy to compare. The Matlab code used to create this plot is located in Appendix C. Using this program and the bearing measurements, the BePerf bearing analysis program for the High Speed Pinion Bearings could be run confidently. A comparison of characteristics between the estimated bearing and measured bearing is shown in Table 4.2.

$C_p = 8$ mils; Preload = 0.75; $\chi = 1.5708$; offset = 1.14

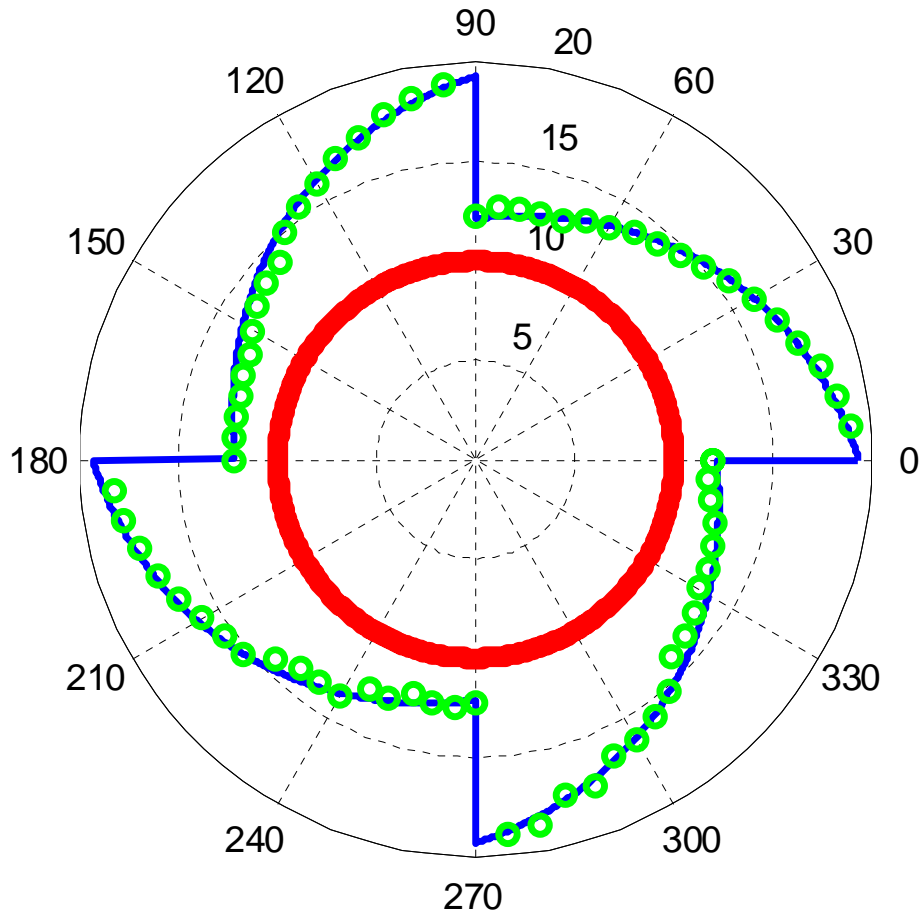


Figure 4.5
Matlab plot used to match measured bearing profile

**Table 4.2 BePerf Approximate and Improved Bearing Properties
N = 25,000 rpm**

	Approximate Profile	Accurate Profile
D	3.75 in	3.75 in
L	2.00 in	1.75 in
Cb	0.003 in	0.00235 in
L/D	0.53	0.4667
Tin	110° F	120° F
Load	75.0 Lbf	75.0 Lbf
Eccen. Ratio	0.026	0.026
Attitude Angle	46.2°	17.85°
Kxx	0.755E+06 Lbf/in	0.1167E+07 Lbf/in
Kxy	0.7E+06 Lbf/in	0.3752E+06 Lbf/in
Kyx	-0.7E+06 Lbf/in	-0.3746E+06 Lbf/in
Kyy	0.758E+06 Lbf/in	0.1167E+07 Lbf/in
Cxx	564 Lbf-sec/in	311.53 Lbf-sec/in
Cxy	-0.147 Lbf-sec/in	-0.2505E-01 Lbf-sec/in
Cyx	-0.147 Lbf-sec/in	-0.2505E-01 Lbf-sec/in
Cyy	564 Lbf-sec/in	311.57 Lbf-sec/in
Lobe Start	55°, 145°, 235°, 325°	10°, 100°, 190°, 280°
Lobe End	125°, 215°, 305°, 395°	80°, 170°, 260°, 350°
Land deg	70°	70°
Preload	0.6	0.75
Offset	0.8	1.14

4.2 Analytical Model Comparison

The CRF test stand bearing loading is calculated using the Visual Basic.Net program shown in Chapter 3. An accurate torque split value must be entered into the program to get useful results. The torque split is analyzed with the analytical method derived in Chapter 3. The stiffness factors in each power path are two of the constants that need to be computed. Table 4.3 shows the stiffness factors of different sections of

each power path. The total stiffness is the equivalent stiffness of multiple springs in series:

$$K_{TOTAL} = \frac{1}{\frac{1}{K_1} + \frac{1}{K_2} + \frac{1}{K_3} + \frac{1}{K_4} + \dots + \frac{1}{K_N}} \quad (4 - 2)$$

Table 4.3 Stiffness Factors in each Path of the CRF test stand

	Stiffness, K (in-lb/rad)	
	PATH A	PATH B
Bull Gear (HSGB3)	86.9 E+6	77.8 E+6
HS Pinion (LSGB)	569 E+6	569 E+6
Quill Shaft		
Shaft	61.0 E+6	61.0 E+6
Coupling Rigid #3	1330 E+6	1330 E+6
Coupling Rigid #4	233 E+6	233 E+6
TOTAL STIFFNESS*	2.882 E+7	2.772 E+7

* Total Stiffness is not a summation. Equation 4-2 is used for total.

The significant difference in geometry between paths A and B is the high speed bull gear. The only other difference is a vernier gear located in Path A. Specifically, the vernier gear is located at the quill shaft coupling near the low speed gear box. This vernier gear allows the operator to change the torque split manually. The gear teeth inside the vernier gear assembly allow the operator to change the angular position of the quill shaft relative to the pinion gear in the low speed gear box. Due to this

arrangement, the four main gear meshes are in contact at all times. This is slightly different than the conceptual model in Figure 3.1 where the clocking angle is a gap at one of the four gear meshes. In the CRF test stand, the clocking angle is measured at the vernier gear coupling. Analytically it does not matter where the clocking angle is measured.

Using the stiffness factors in Table 4.3, the torque in each path was calculated and plotted. Figure 4.6 shows the torque in each path as the total input torque is increased from zero. A clocking angle of 0.03 radians was used for this plot. The system horsepower changes drastically depending on the turbo machinery equipment being tested. The input power for the CRF test stand is between 5,000 HP and 15,000 HP under most operating conditions. Figure 4.6 points out the difference in torque between path A and path B with an input of 10,000 HP. Horsepower (HP) is related to torque (in-lb) using the following equation:

$$\text{Input Torque} = \frac{HP \times 63024}{RPM} \quad (\text{in - lbs})$$

Figure's 4.7 and 4.8 show the effects of increasing the clocking angle. Figure 4.7 was generated using Equation 4-6 while fixing the Total Input Torque as a constant. The plot in Figure 4.8 was generated using Equations 4-3 and 4-5. Using these plots, the operator at the CRF can chose the appropriate clocking angle for the vernier gear.

Figure 4.9 shows the final bearing parameters and the BePerf model. Notice the load vector, W , is not in the direction of gravity. The resultant bearing load is entered into BePerf directly from the Gearbox Bearing Loads Visual Basic.NET program.

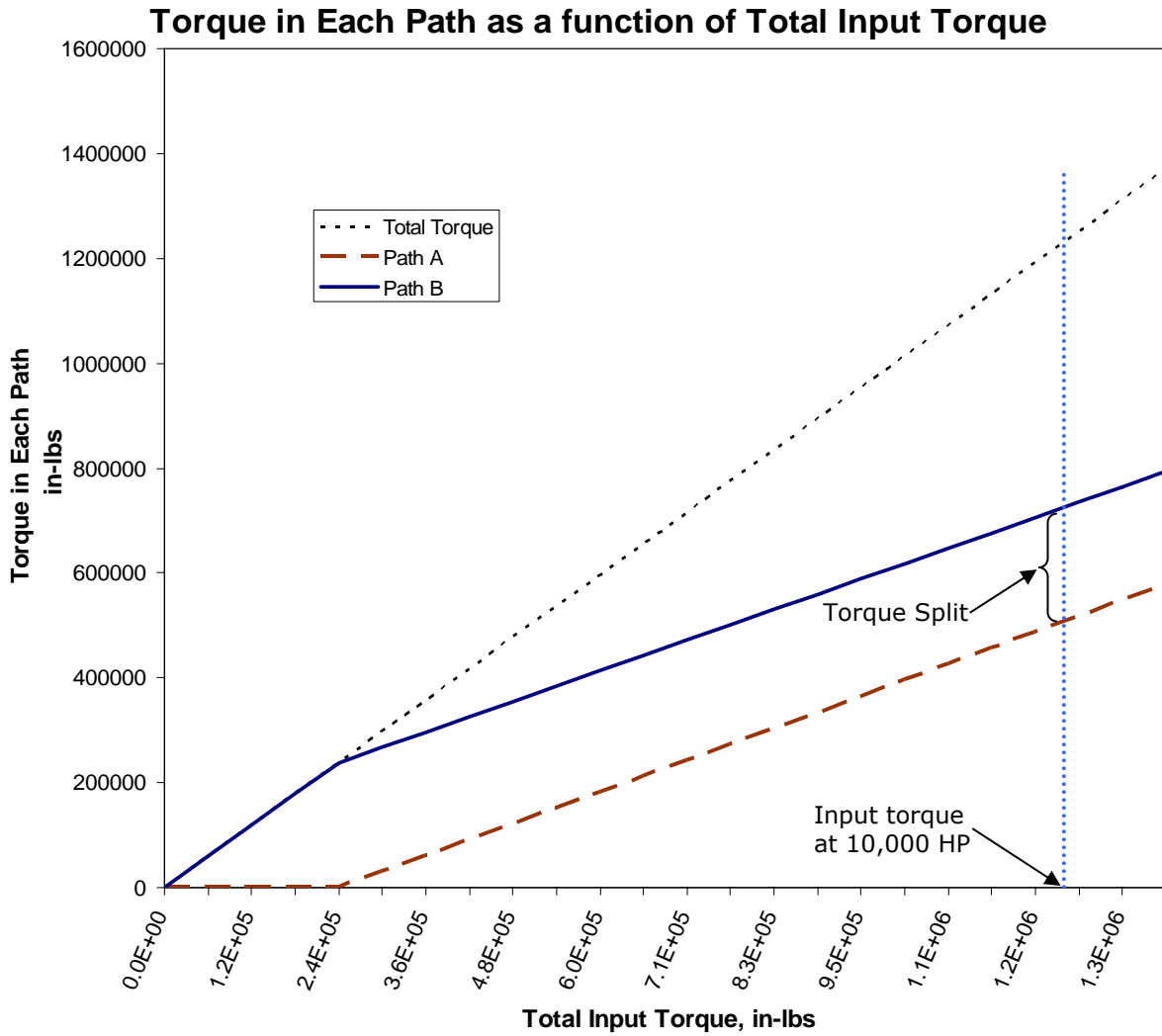


Figure 4.6
 Torque split plot using the CRF gear train parameters
 $\beta = 0.03$ radians , $GR = .286549$
 $K_A = 28820000$ in-lbs/rad , $K_B = 27720000$ in-lbs/rad

Torque Split as a Function of Clocking Angle

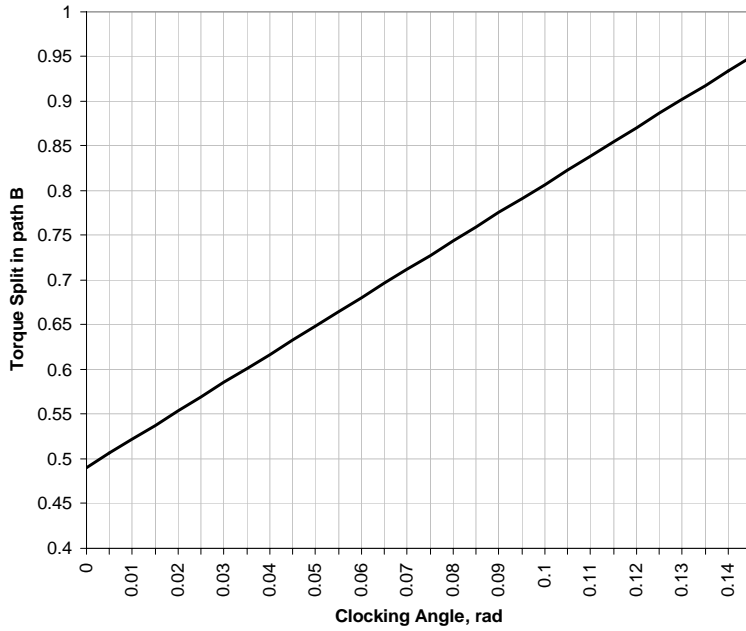


Figure 4.7
 Torque Split in Path B as a Function of Clocking Angle
 CRF gear train parameters
 Total Input Torque = 1278000 in-lbs , GR = .286549

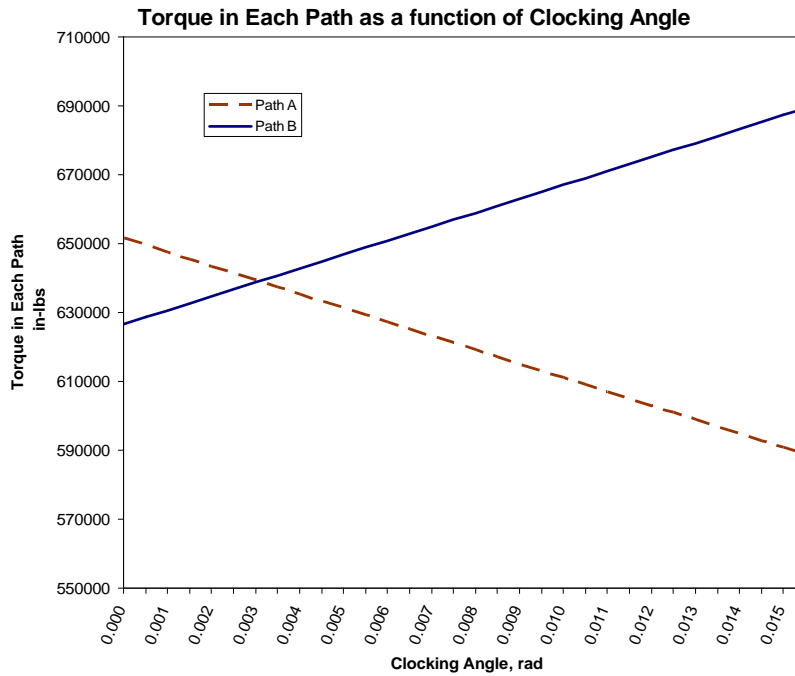


Figure 4.8
 Torque in Each path as a Function of Clocking Angle
 Total Input Torque = 1278000 in-lbs , GR = .286549
 $K_A = 28820000$ in-lbs/rad , $K_B = 27720000$ in-lbs/rad

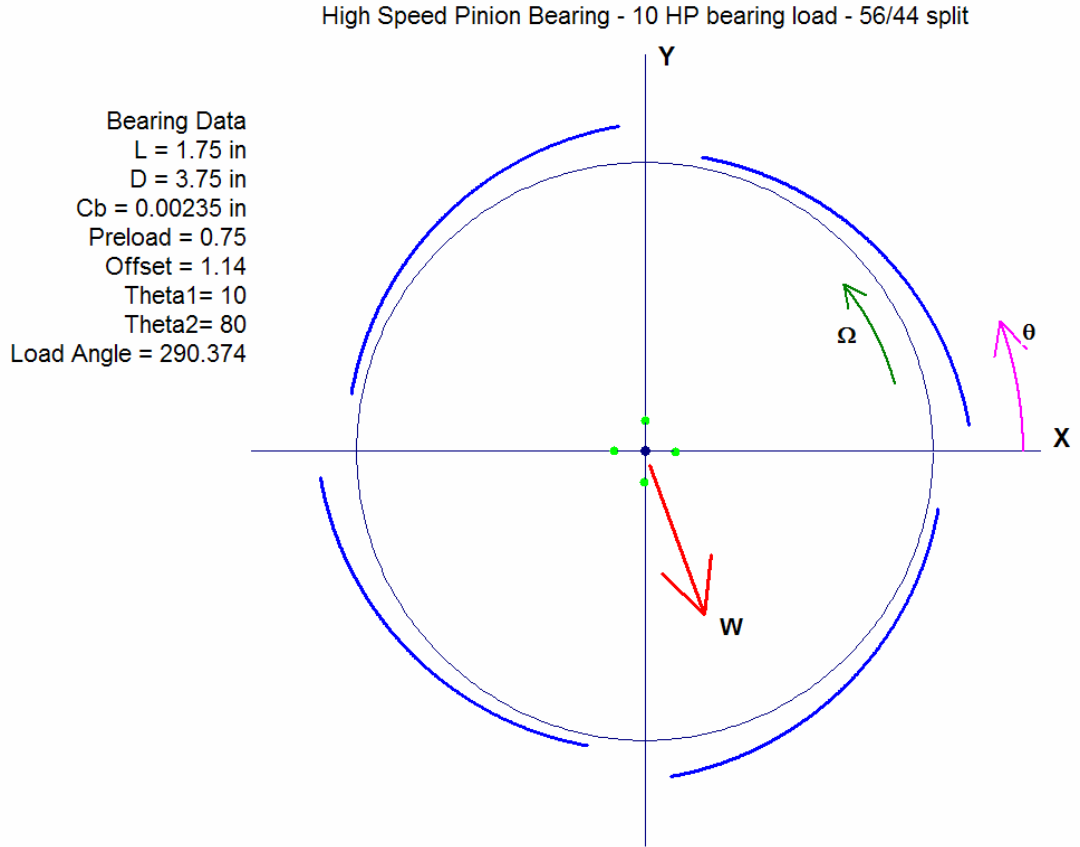


Figure 4.9
 BePerf Bearing Diagram Updated with Correct Loading Vector

Figure 4.10 shows the forced response of the H.S. Pinion with the correct bearing profiles and bearing loading vector. A Total Input Torque of 1278000 in-lbs is used for most of the analyses run on the DyRoBeS model. This is a likely value based on data taken from the CRF. Note the differences between the estimated model used in Figure 4.3 and the accurate model used in Figure 4.10. There is no backward whirl predicted from the forced response analysis of the high speed train. Figure 4.11 shows the forced response in a 3D orbit view. This analysis was done using a horsepower of 10,000.

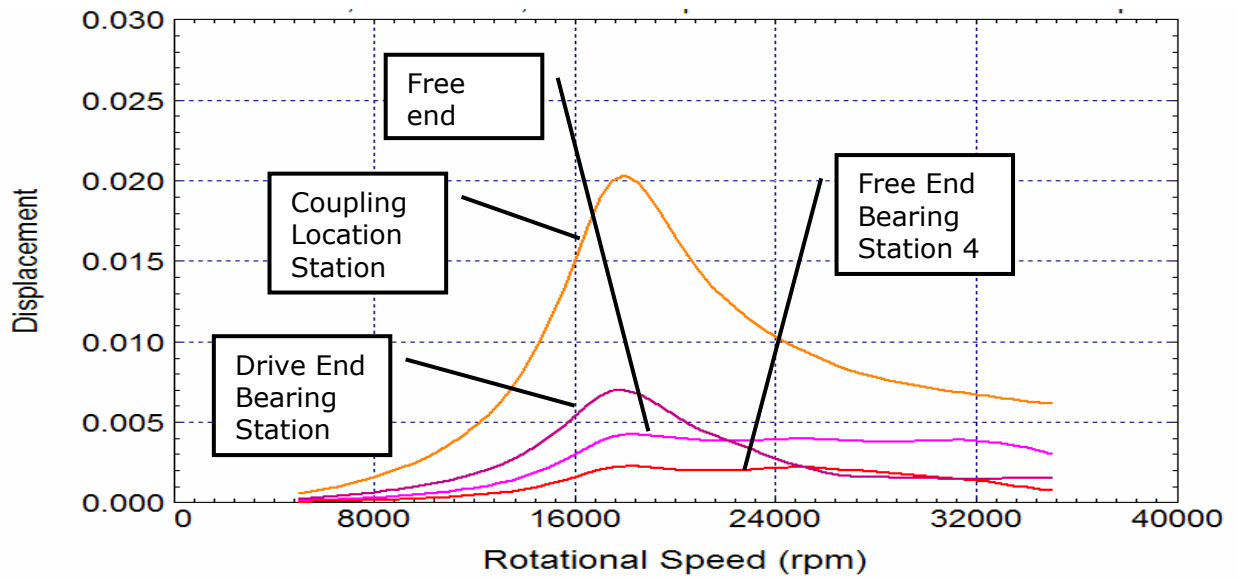


Figure 4.10
 Multiple Station Forced Response
 Total Input Torque = 1278000 in-lbs
 10,000 Horsepower

Shaft Response - due to shaft 1 excitation
 Rotor Speed = 25000 rpm, Response - FORWARD Precession
 Max Orbit at stn 18, substn 1, with $a = 0.0048556$, $b = 0.0047942$

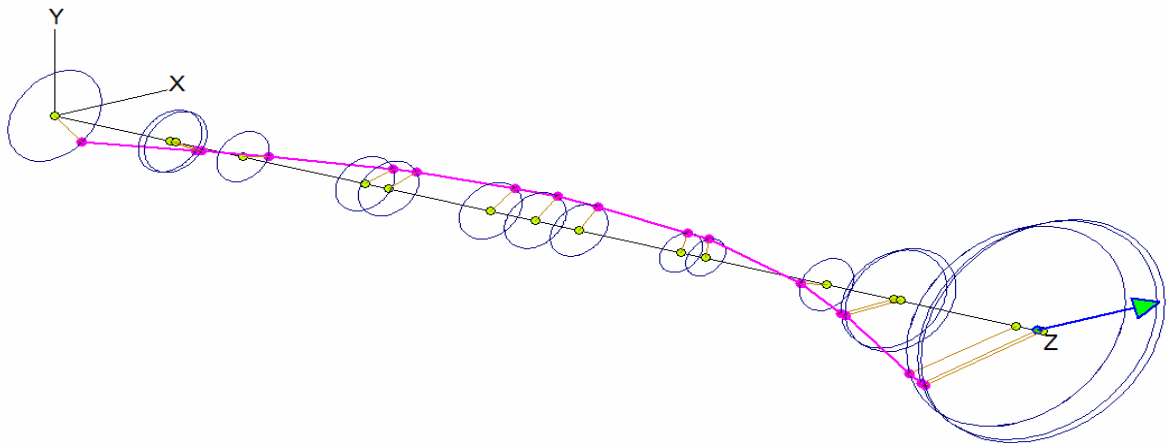


Figure 4.11
 3D Forced Response
 10,000 HP, 0.56 Torque Split

Sensitivity plots are useful for seeing the effects of changing parameters in a model. Figure 4.12 is a sensitivity plot that compares the effects due to changes in bearing support stiffness. The bearing support stiffness can also be thought of as the gearbox shell or frame stiffness. Note how the response magnitude increases as the support stiffness decreases. In addition, the critical speed decreases as the stiffness decreases. It is desirable to have a very stiff support or frame on this gearbox. There is no data from the CRF that indicates the actual stiffness of the gearbox. The results from the sensitivity plot in Figure 4.12 are summarized in Table 4.4. Figure 4.13 is a plot of the sensitivity to changes in bearing load. Bearing load can be changed by altering the torque split on the quill shafts. There is not much difference in response until the torque split is very drastic (70/30). Although a torque split of 0.70 is considered drastic, a torque split of .73 was run on the CRF test stand at one point during testing. The results from the sensitivity plot in Figure 4.13 are summarized in Table 4.5.

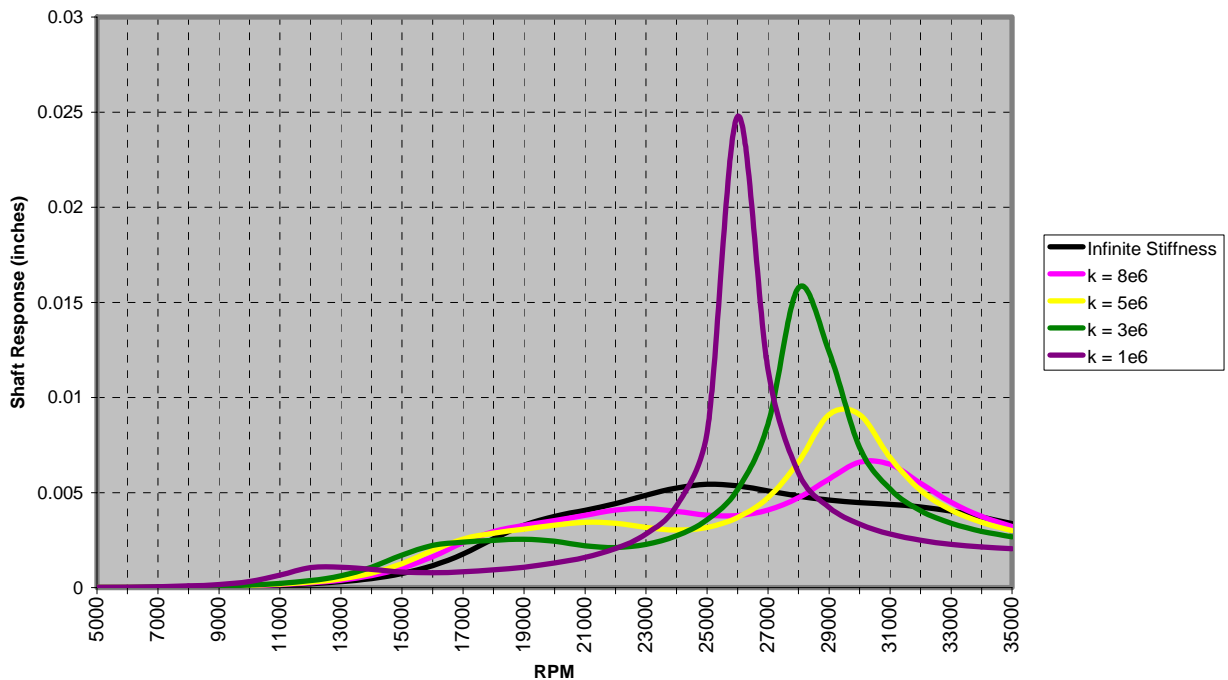


Figure 4.12
Sensitivity Plot – Changes in Support Stiffness
Peak-to-peak Response – Station 12 of DyRoBeS Model

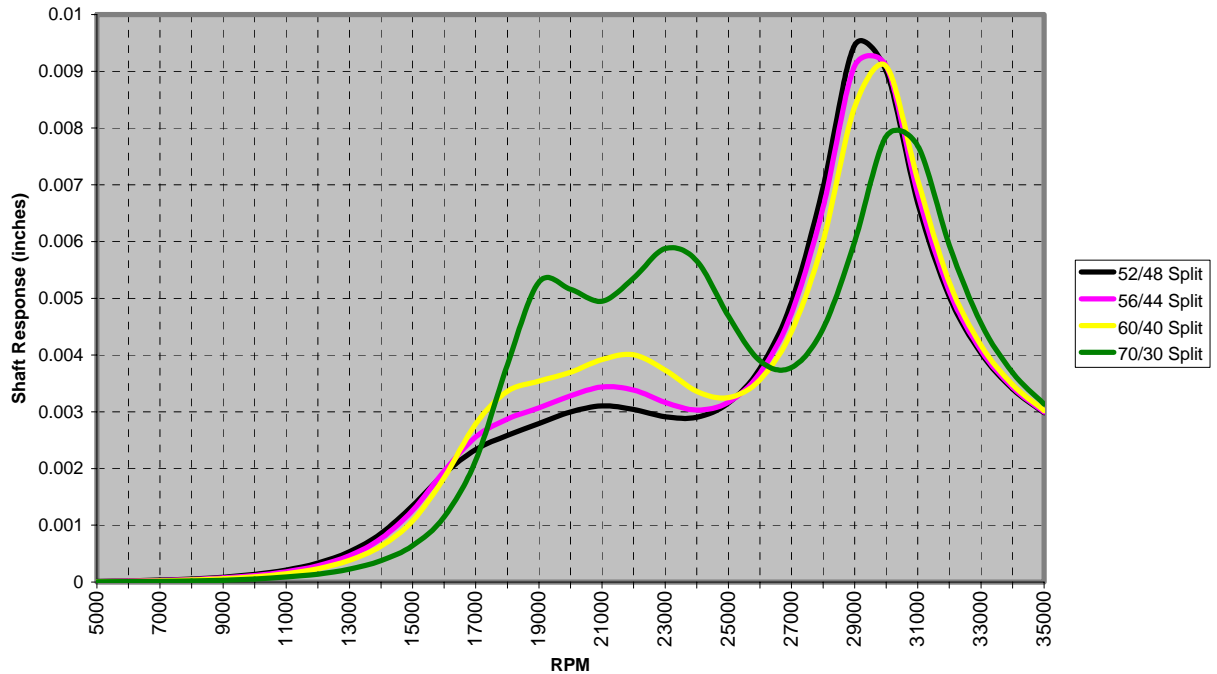


Figure 4.13
Sensitivity Plot - Changes in Torque Splits
Peak-to-Peak Response- Station 12 of DyRoBeS Model

Table 4.4
Bearing Support Stiffness Sensitivity (Pedestal Stiffness)

Stiffness	Infinite Stiffness	k = 8e6 lb/in	k = 5e6 lb/in	k = 3e6 lb/in	k = 1e6 lb/in
Peak Response Speed (rpm)	25,000	30,000	29,500	28,000	26,000
Response Magnitude	0.006	0.007	0.009	0.016	0.025

Table 4.5
Bearing Load Sensitivity (Adjustment of Torque Split)

Torque Split	52/48	56/44	60/40	70/30
Peak Response Speed (rpm)	29,000	29,500	30,000	30,500
Response Magnitude	0.0095	0.0093	0.0091	0.008

Chapter 5

Conclusions and Recommendations

5.1 Conclusions

The purpose of this investigation was to better understand split path transmission load sharing. This knowledge has been and will continue to be used to analyze the CRF drive system gearboxes in order to reduce excessive vibration. The following two conclusions are based on the split path concepts in Chapter 3:

- The torque split is not affected by the stiffness or windup of any sections (shafts, gears, bearings, etc.) outside of the two split power paths.
- If the stiffness factors of both paths are the same, the difference in torque between the two paths does not change as the total input torque increases. The slope of the two paths are identical.

The following conclusions result from the CRF drive system analysis:

- There is no backward whirl predicted from the forced response analysis of the high speed train.
- The forced response is very sensitive to changes of stiffness in the HSGB III pinion bearing supports. Higher stiffness is desirable as it raises the critical speed and lowers the vibration amplitudes of the pinion bending mode.
- HSGB III pinion analysis has revealed several well damped modes in the operating speed range. One suspect mode is a pinion free-free mode that is very sensitive to bearing pedestal flexibility and amplifies if the pedestal stiffness is reduced from a typical rigid assumption.

- Increasing the pinion bearing load by changing the gear torque split lowers the vibration levels by only 16% for the highest load considered.
- Increasing the pinion bearing load is predicted to raise the pinion bending critical speed by only 1500 rpm for the highest load considered.

5.2 Recommendations

From the experience of this research, the following recommendations on future work are suggested:

- Consider the gear tooth stiffness in split path gear train analysis. This would decrease the stiffness factor of each path. In the case considered in this report the gear tooth stiffness was insignificant. Gear tooth stiffness may have a significant impact on the path stiffness factors in a split path transmission with no quill shafts.
- Improve the *Gearbox Bearing Loads* program by adding the capability to arrange the gear shafts beyond the 90 degree relative position.
- Investigate the possible occurrence of synchronous thermal instability produced by the current lightly loaded 4-lobe drive end bearing.
- Design a tilting pad bearing for optimum performance to replace the current fixed geometry insert bearing on the HSGB III pinion shaft.
- Investigate the possible occurrence of synchronous thermal instability produced by the new tilting pad bearing design on the drive end pinion bearing location.
- Additional detailed examination of the HSGB III gear and pinion vibration, from actual runs and/or taped data, is required to better identify the characteristics of the high vibration excursions.

- Investigate other possible thermal instability sources in high speed and high load double helical gear designs.

References

- [1] Szeri, A.Z. *Fluid Film Lubrication: Theory and Design*, Cambridge University Press, Cambridge, UK, 1998.
- [2] Balena, F. *Programming Microsoft Visual Basic.Net : Core Reference*, Microsoft Press, Redmond, WA, 2002
- [3] Krantz, T.L. *A Method to Analyze and Optimize the Load Sharing of Split-Path Transmissions*. Proceedings of the 7th International Power Transmission and Gearing Conference, San Diego, CA, October, 1996, pp. 227-237.
- [4] Krantz, T.L., Rashidi, M. and Kish, J.G. *Split Torque Transmission Load Sharing*. Proceedings of the “Gearbox Configurations of the 90’s”. Institute of Mechanical Engineers, Solihull, West Midlands, UK, October 28, 1992.
- [5] Rashidi, M. *Dynamics of a Split Torque Helicopter Transmission*. Proceedings of the International Power Transmission and Gearing Conference, Scottsdale, AZ, September, 1992, pp. 347-358.
- [6] White, G. *Design Study of a Split-Torque Helicopter Transmission*. Proceedings of the Institution of Mechanical Engineers, Vol 212, part G, IMechE 1998.
- [7] Smith, J.D. *Gears and Their Vibration: A Basic Approach to Understanding Gear Noise*. Marcel Dekker, Inc., New York, NY, 1983.
- [8] Litvin, F.L. *Gear Geometry and Applied Theory*, Prentice-Hall, Inc., Englewood Cliffs, NJ, 1994.
- [9] W. J. Chen. *DyRoBeS_Rotor*, Version 8.0, [Computer Program]. Eigen Technologies, Inc., 2003.
- [10] Kirk, R.G. *VT-FAST*, Version 2.0, [Computer Program]. Mechanical Engineering Department, Virginia Tech, 1997.
- [11] W. J. Chen. *DyRoBeS_BePerf*, Version 8.0, [Computer Program]. Eigen Technologies, Inc., 2003.
- [12] MathWorks, 2001, *MATLAB*, ver. 6, rel 12, [Computer program]. Available Distributor: The MathWorks Inc., 24 Prime Park Way, Natick, MA, 01760-1500, USA.

Appendix A

Gearbox Bearing Loads: Gear Layout 1
Visual Basic.NET Code Segment

' This Subroutine is for Gear Layout 1

```
Sub LoadCalc1(ByVal HP As Double, ByVal RPM As Double, ByVal torque_ratio As Double, _  
    ByVal pd0 As Double, ByVal pd1 As Double, _  
    ByVal pn1 As Double, ByVal pn2 As Double, ByVal hel_deg1 As Double, ByVal hel_deg2 As Double, _  
    ByVal phiN_deg1 As Double, ByVal phiN_deg2 As Double, ByVal N1 As Double, _  
    ByVal N2 As Double, ByVal Theta As Single, ByVal BearingDistA As Double, _  
    ByVal BearingDistB As Double, ByVal BearingDistC As Double, _  
    ByVal BearingDistD As Double, ByVal WeightA As Single, ByVal WeightB As Single, _  
    ByVal WeightC As Single, ByVal WeightD As Single, _  
    ByVal singlehelical As Boolean, ByVal oneGLoadYes As Boolean, ByVal pdknown As Boolean, _  
    ByVal SiChecked As Boolean, ByVal HelixDirection1 As String)
```

```
Dim pn(2), N(2), phiN_deg(2), phiT_rad(2), hel_deg(2), i As Double  
Dim pd(2), phiN_rad, hel_rad, input_torque, torque1, torque3 As Double  
Dim F21_t, F21_r, F21_a, F12_t, F12_r, F12_a, H, Direction As Double  
Dim R_2C(2, 0), R_DC(2, 0), F12(2, 0), R_1A(2, 0), R_BA(2, 0), F21(2, 0), _  
R_2C_x_F12(2, 0), R_DC_x_F12(2, 0), R_1A_x_F21(2, 0), R_BA_x_F21(2, 0) As Double  
Dim pi As Double = Math.PI
```

' Gear 1 parameters

```
pn(0) = pn1          ' The normal diametral pitch  
N(0) = N1           ' The number of teeth  
phiN_deg(0) = phiN_deg1 ' The normal pressure angle (degrees)  
hel_deg(0) = hel_deg1 ' The helix angle (degrees)  
pd(0) = pd0        ' The pitch diameter (if known)
```

' Gear 2 parameters

```
pn(1) = pn2  
N(1) = N2  
phiN_deg(1) = phiN_deg2  
hel_deg(1) = hel_deg2  
pd(1) = pd1
```

' Convert from SI to Standard if Necessary

```
If SiChecked = True Then  
    BearingDistA = BearingDistA * 39.3700787  
    BearingDistB = BearingDistB * 39.3700787  
    BearingDistC = BearingDistC * 39.3700787  
    BearingDistD = BearingDistD * 39.3700787
```

```
WeightA = WeightA * 2.2046226  
WeightB = WeightB * 2.2046226  
WeightC = WeightC * 2.2046226  
WeightD = WeightD * 2.2046226
```

```
For i = 0 To 1  
    pd(i) = pd(i) * 39.3700787  
    pn(i) = (25.4 / pn(i))  
Next
```

End If

' Find out which options are chosen by the user

```
If singlehelical = False Then  
    hel_deg(0) = 0  
    hel_deg(1) = 0  
End If
```

If pdknown = False Then

```
pd(0) = N(0) / (pn(0) * Cos(hel_deg(0) * pi / 180)) ' Pitch diameter for gear 1  
pd(1) = N(1) / (pn(1) * Cos(hel_deg(1) * pi / 180)) ' Pitch diameter for gear 2  
End If
```

```

' Check Helix Direction
If HelixDirection1 = "Right Hand" And singlehelical = True Then
    H = -1
Else
    H = 1
End If

' Check Rotation Direction
If RPM > 0 Then
    Direction = 1
Else
    Direction = -1
End If

' Transverse pressure angles for gears 1 and 2 (radians)
phiT_rad(0) = Atan((Tan(phiN_deg(0) * pi / 180)) / (Cos(hel_deg(0) * pi / 180)))
phiT_rad(1) = Atan((Tan(phiN_deg(1) * pi / 180)) / (Cos(hel_deg(1) * pi / 180)))

' Calculate Torque split from horsepower and speed
input_torque = Abs((HP * 5252 / RPM) * 12)
RPM2 = (RPM / (N1 / N2))

' Force Calculations

F12_t = input_torque / ((pd(0)) / 2)
F12_r = F12_t * Tan(phiT_rad(0))
F12_a = H * F12_t * Tan(hel_deg(0) * pi / 180)

Dim F12_tx As Double = -Direction * F12_t * Sin(Theta * pi / 180)
Dim F12_ty As Double = Direction * F12_t * Cos(Theta * pi / 180)
Dim F12_rx As Double = F12_r * Cos(Theta * pi / 180)
Dim F12_ry As Double = F12_r * Sin(Theta * pi / 180)

F21_a = -F12_a
Dim F21_tx As Double = -F12_tx
Dim F21_ty As Double = -F12_ty
Dim F21_rx As Double = -F12_rx
Dim F21_ry As Double = -F12_ry

' Moment Balance about Bearing C
R_2C(0, 0) = (-pd(1) / 2) * Cos(Theta * pi / 180)
R_2C(1, 0) = (-pd(1) / 2) * Sin(Theta * pi / 180)
R_2C(2, 0) = -BearingDistC
R_DC(0, 0) = 0
R_DC(1, 0) = 0
R_DC(2, 0) = -(BearingDistC + BearingDistD)

F12(0, 0) = F12_rx + F12_tx : F12(1, 0) = F12_ty + F12_ry : F12(2, 0) = F12_a

' Moment Balance about Bearing A
R_1A(0, 0) = (pd(0) / 2) * Cos(Theta * pi / 180)
R_1A(1, 0) = (pd(0) / 2) * Sin(Theta * pi / 180)
R_1A(2, 0) = -BearingDistA
R_BA(0, 0) = 0
R_BA(1, 0) = 0
R_BA(2, 0) = -(BearingDistA + BearingDistB)

F21(0, 0) = F21_rx + F21_tx : F21(1, 0) = F21_ty + F21_ry : F21(2, 0) = F21_a

'Multiply Vectors
R_2C_x_F12 = cross(R_2C, F12)
R_1A_x_F21 = cross(R_1A, F21)

' X and Y Force components on Bearing D
Fy(3) = R_2C_x_F12(0, 0) / -(BearingDistC + BearingDistD)

```

```

Fx(3) = R_2C_x_F12(1, 0) / (BearingDistC + BearingDistD)

' X and Y Force components on Bearing B
Fy(1) = R_1A_x_F21(0, 0) / -(BearingDistA + BearingDistB)
Fx(1) = R_1A_x_F21(1, 0) / (BearingDistA + BearingDistB)

' Solve for remaining components

Fx(2) = -F12(0, 0) - Fx(3)
Fy(2) = -F12(1, 0) - Fy(3)
Fz(2) = -F12(2, 0)
Fz(3) = Fz(2)

Fx(0) = -F21(0, 0) - Fx(1)
Fy(0) = -F21(1, 0) - Fy(1)
Fz(0) = -F21(2, 0)
Fz(1) = -Fz(0)

For i = 0 To 3
    Fy(i) = -Fy(i)
    Fx(i) = -Fx(i)
Next

'Check to see if the user chose the 1G load option
If oneGLoadYes = True Then
    Fy(0) = Fy(0) - WeightA
    Fy(1) = Fy(1) - WeightB
    Fy(2) = Fy(2) - WeightC
    Fy(3) = Fy(3) - WeightD
End If

' Calculate Resultant vectors

R(0) = Sqrt(Fy(0) ^ 2 + Fx(0) ^ 2)
R(1) = Sqrt(Fy(1) ^ 2 + Fx(1) ^ 2)
R(2) = Sqrt(Fy(2) ^ 2 + Fx(2) ^ 2)
R(3) = Sqrt(Fy(3) ^ 2 + Fx(3) ^ 2)

Angle_deg(0) = (Acos(Abs(Fy(0)) / R(0))) * 180 / pi
Angle_deg(1) = (Acos(Abs(Fy(1)) / R(1))) * 180 / pi
Angle_deg(2) = (Acos(Abs(Fy(2)) / R(2))) * 180 / pi
Angle_deg(3) = (Acos(Abs(Fy(3)) / R(3))) * 180 / pi

' Convert Results back to SI if necessary
If SiChecked = True Then

    For i = 0 To 3
        Fx(i) = Fx(i) * 4.4482216
        Fy(i) = Fy(i) * 4.4482216
    Next

    For i = 0 To 1
        Fz(i) = Fz(i) * 4.4482216
    Next
End If

End Sub

```

Appendix B

Gearbox Bearing Loads: Gear Layout 2
Visual Basic.NET Code Segment

```
' Gear 1 parameters
pn(0) = pn1      ' The normal diametral pitch
N(0) = N1        ' The number of teeth
phiN_deg(0) = phiN_deg1  ' The normal pressure angle (degrees)
hel_deg(0) = hel_deg1  ' The helix angle (degrees)
pd(0) = pd0      ' Pitch Diameter
```

```
' Gear 2 parameters
pn(1) = pn2
N(1) = N2
phiN_deg(1) = phiN_deg2
hel_deg(1) = hel_deg2
pd(1) = pd1
```

```
' Gear 3 parameters
pn(2) = pn3
N(2) = N3
phiN_deg(2) = phiN_deg3
hel_deg(2) = hel_deg3
pd(2) = pd2
```

```
' Gear 4 parameters
pn(3) = pn4
N(3) = N4
phiN_deg(3) = phiN_deg4
hel_deg(3) = hel_deg4
pd(3) = pd3
```

```
' Gear 5 parameters
pn(4) = pn5
N(4) = N5
phiN_deg(4) = phiN_deg5
hel_deg(4) = hel_deg5
pd(4) = pd4
```

```
' Gear 6 parameters
pn(5) = pn6
N(5) = N6
phiN_deg(5) = phiN_deg6
hel_deg(5) = hel_deg6
pd(5) = pd5
```

```
' Convert from SI to Standard if Necessary
If SiChecked = True Then
```

```
    BearingDistA = BearingDistA * 39.3700787
    BearingDistB = BearingDistB * 39.3700787
    BearingDistC = BearingDistC * 39.3700787
    BearingDistD = BearingDistD * 39.3700787
    BearingDistE = BearingDistE * 39.3700787
    BearingDistF = BearingDistF * 39.3700787
    BearingDistG = BearingDistG * 39.3700787
    BearingDistH = BearingDistH * 39.3700787
    BearingDistI = BearingDistI * 39.3700787
    BearingDistJ = BearingDistJ * 39.3700787
    BearingDistK = BearingDistK * 39.3700787
    BearingDistL = BearingDistL * 39.3700787
```

```
WeightA = WeightA * 2.2046226
WeightB = WeightB * 2.2046226
WeightC = WeightC * 2.2046226
WeightD = WeightD * 2.2046226
WeightE = WeightE * 2.2046226
WeightF = WeightF * 2.2046226
WeightG = WeightG * 2.2046226
WeightH = WeightH * 2.2046226
WeightI = WeightI * 2.2046226
```

```

WeightJ = WeightJ * 2.2046226
WeightK = WeightK * 2.2046226
WeightL = WeightL * 2.2046226

For i = 0 To 5
    pd(i) = pd(i) * 39.3700787
    pn(i) = (25.4 / pn(i))
Next

End If

' Find out which gear type the user chose

If singlehelical = False Then
    hel_deg(0) = 0
    hel_deg(1) = 0
    hel_deg(2) = 0
    hel_deg(3) = 0
    hel_deg(4) = 0
    hel_deg(5) = 0
End If

' Pitch Diameter Calculations
If pdknown = False Then
    For i = 0 To 5
        pd(i) = N(i) / (pn(i) * Cos(hel_deg(i) * pi / 180))
    Next
End If

' Check Helix Direction
If HelixDirection2 = "Right Hand" And singlehelical = True Then
    H2 = -1
Else
    H2 = 1
End If

If HelixDirection5 = "Left Hand" And singlehelical = True Then
    H5 = -1
Else
    H5 = 1
End If

' Check Rotation Direction
If RPM > 0 Then
    Direction = 1
Else
    Direction = -1
End If

' Transverse pressure angles for gears 1 and 2 (radians)
For i = 0 To 5
    phiT_rad(i) = Atan((Tan(phiN_deg(i) * pi / 180)) / (Cos(hel_deg(i) * pi / 180)))
Next

' Calculate Torque split from horsepower and speed
input_torque1 = Abs((HP * 5252 / RPM) * 12)
RPM2 = (RPM / (N1 / N2))
input_torque2 = Abs((HP * 5252 / RPM2) * 12)
torque1 = torque_ratio * input_torque1
torque3 = (1 - torque_ratio) * input_torque1
torque4 = torque_ratio * input_torque2
torque6 = (1 - torque_ratio) * input_torque2

' Force Calculations

' Force on gear 1 from gear 2

```

```

F21_t = torque1 / ((pd(1)) / 2)
F21_r = F21_t * Tan(phiT_rad(1))
F21_a = H2 * F21_t * Tan(hel_deg(1)) * pi / 180

Dim F21_tx As Double = Direction * F21_t * Sin(Theta1 * pi / 180)
Dim F21_ty As Double = -Direction * F21_t * Cos(Theta1 * pi / 180)
Dim F21_rx As Double = -F21_r * Cos(Theta1 * pi / 180)
Dim F21_ry As Double = -F21_r * Sin(Theta1 * pi / 180)

' Force on gear 2 from gear 1
F12_a = -F21_a
Dim F12_tx As Double = -F21_tx
Dim F12_ty As Double = -F21_ty
Dim F12_rx As Double = -F21_rx
Dim F12_ry As Double = -F21_ry

' Force on gear 3 from gear 2
Dim F23_t As Double = torque3 / ((pd(1)) / 2)
Dim F23_r As Double = F23_t * Tan(phiT_rad(1))
Dim F23_a As Double = H2 * F23_t * Tan(hel_deg(1)) * pi / 180

Dim F23_tx As Double = Direction * F23_t * Sin(Theta1 * pi / 180)
Dim F23_ty As Double = Direction * F23_t * Cos(Theta1 * pi / 180)
Dim F23_rx As Double = F23_r * Cos(Theta1 * pi / 180)
Dim F23_ry As Double = -F23_r * Sin(Theta1 * pi / 180)

' Force on gear 2 from gear 3
Dim F32_a = -F23_a
Dim F32_tx As Double = -F23_tx
Dim F32_ty As Double = -F23_ty
Dim F32_rx As Double = -F23_rx
Dim F32_ry As Double = -F23_ry

' Force on gear 5 from gear 4
Dim F45_t As Double = torque4 / ((pd(3)) / 2)
Dim F45_r As Double = F45_t * Tan(phiT_rad(3))
Dim F45_a As Double = H5 * F45_t * Tan(hel_deg(3)) * pi / 180

Dim F45_tx As Double = Direction * F45_t * Sin(Theta2 * pi / 180)
Dim F45_ty As Double = -Direction * F45_t * Cos(Theta2 * pi / 180)
Dim F45_rx As Double = F45_r * Cos(Theta2 * pi / 180)
Dim F45_ry As Double = F45_r * Sin(Theta2 * pi / 180)

' Force on gear 4 from gear 5
Dim F54_a = -F45_a
Dim F54_tx As Double = -F45_tx
Dim F54_ty As Double = -F45_ty
Dim F54_rx As Double = -F45_rx
Dim F54_ry As Double = -F45_ry

' Force on gear 5 from gear 6
Dim F65_t As Double = torque6 / ((pd(5)) / 2)
Dim F65_r As Double = F65_t * Tan(phiT_rad(5))
Dim F65_a As Double = H5 * F65_t * Tan(hel_deg(5)) * pi / 180

Dim F65_tx As Double = Direction * F65_t * Sin(Theta2 * pi / 180)
Dim F65_ty As Double = Direction * F65_t * Cos(Theta2 * pi / 180)
Dim F65_rx As Double = -F65_r * Cos(Theta2 * pi / 180)
Dim F65_ry As Double = F65_r * Sin(Theta2 * pi / 180)

' Force on gear 6 from gear 5
Dim F56_a = -F65_a
Dim F56_tx As Double = -F65_tx
Dim F56_ty As Double = -F65_ty
Dim F56_rx As Double = -F65_rx
Dim F56_ry As Double = -F65_ry

' Moment Balance about Bearing A

```

$R_{1A}(0, 0) = (pd(0) / 2) * \cos(\text{Theta1} * \pi / 180)$
 $R_{1A}(1, 0) = (pd(0) / 2) * \sin(\text{Theta1} * \pi / 180)$
 $R_{1A}(2, 0) = -\text{BearingDistA}$
 $R_{BA}(0, 0) = 0$
 $R_{BA}(1, 0) = 0$
 $R_{BA}(2, 0) = -(\text{BearingDistA} + \text{BearingDistB})$

$F21(0, 0) = F21_{rx} + F21_{tx} : F21(1, 0) = F21_{ty} + F21_{ry} : F21(2, 0) = F21_a$

' Moment Balance about Bearing C

$R_{2Cfrom1}(0, 0) = (-pd(1) / 2) * \cos(\text{Theta1} * \pi / 180)$
 $R_{2Cfrom1}(1, 0) = (-pd(1) / 2) * \sin(\text{Theta1} * \pi / 180)$
 $R_{2Cfrom1}(2, 0) = -\text{BearingDistC}$
 $R_{2Cfrom3}(0, 0) = (pd(1) / 2) * \cos(\text{Theta1} * \pi / 180)$
 $R_{2Cfrom3}(1, 0) = (pd(1) / 2) * \sin(\text{Theta1} * \pi / 180)$
 $R_{2Cfrom3}(2, 0) = -\text{BearingDistC}$
 $R_{DC}(0, 0) = 0$
 $R_{DC}(1, 0) = 0$
 $R_{DC}(2, 0) = -(\text{BearingDistC} + \text{BearingDistD})$

$F12(0, 0) = F12_{rx} + F12_{tx} : F12(1, 0) = F12_{ty} + F12_{ry} : F12(2, 0) = F12_a$
 $F32(0, 0) = F32_{rx} + F32_{tx} : F32(1, 0) = F32_{ty} + F32_{ry} : F32(2, 0) = F32_a$

' Moment Balance about Bearing E

$R_{3E}(0, 0) = (-pd(2) / 2) * \cos(\text{Theta1} * \pi / 180)$
 $R_{3E}(1, 0) = (pd(2) / 2) * \sin(\text{Theta1} * \pi / 180)$
 $R_{3E}(2, 0) = -\text{BearingDistE}$
 $R_{FE}(0, 0) = 0$
 $R_{FE}(1, 0) = 0$
 $R_{FE}(2, 0) = -(\text{BearingDistE} + \text{BearingDistF})$

$F23(0, 0) = F23_{rx} + F23_{tx} : F23(1, 0) = F23_{ty} + F23_{ry} : F23(2, 0) = F23_a$

' Moment Balance about Bearing G

$R_{4G}(0, 0) = (pd(3) / 2) * \cos(\text{Theta2} * \pi / 180)$
 $R_{4G}(1, 0) = (pd(3) / 2) * \sin(\text{Theta2} * \pi / 180)$
 $R_{4G}(2, 0) = -\text{BearingDistG}$
 $R_{HG}(0, 0) = 0$
 $R_{HG}(1, 0) = 0$
 $R_{HG}(2, 0) = -(\text{BearingDistG} + \text{BearingDistH})$

$F54(0, 0) = F54_{rx} + F54_{tx} : F54(1, 0) = F54_{ty} + F54_{ry} : F54(2, 0) = F54_a$

' Moment Balance about Bearing I

$R_{5Ifrom4}(0, 0) = (-pd(4) / 2) * \cos(\text{Theta2} * \pi / 180)$
 $R_{5Ifrom4}(1, 0) = (-pd(4) / 2) * \sin(\text{Theta2} * \pi / 180)$
 $R_{5Ifrom4}(2, 0) = -\text{BearingDistI}$
 $R_{5Ifrom6}(0, 0) = (pd(4) / 2) * \cos(\text{Theta2} * \pi / 180)$
 $R_{5Ifrom6}(1, 0) = (pd(4) / 2) * \sin(\text{Theta2} * \pi / 180)$
 $R_{5Ifrom6}(2, 0) = -\text{BearingDistI}$
 $R_{JI}(0, 0) = 0$
 $R_{JI}(1, 0) = 0$
 $R_{JI}(2, 0) = -(\text{BearingDistI} + \text{BearingDistJ})$

$F45(0, 0) = F45_{rx} + F45_{tx} : F45(1, 0) = F45_{ty} + F45_{ry} : F45(2, 0) = F45_a$
 $F65(0, 0) = F65_{rx} + F65_{tx} : F65(1, 0) = F65_{ty} + F65_{ry} : F65(2, 0) = F65_a$

' Moment Balance about Bearing K

$R_{6K}(0, 0) = (-pd(5) / 2) * \cos(\text{Theta2} * \pi / 180)$
 $R_{6K}(1, 0) = (pd(5) / 2) * \sin(\text{Theta2} * \pi / 180)$
 $R_{6K}(2, 0) = -\text{BearingDistK}$
 $R_{LK}(0, 0) = 0$

$R_{LK}(1, 0) = 0$
 $R_{LK}(2, 0) = -(\text{BearingDistK} + \text{BearingDistL})$
 $F56(0, 0) = F56_{rx} + F56_{tx} : F56(1, 0) = F56_{ty} + F56_{ry} : F56(2, 0) = F56_a$

*Multiply Vectors

$R_{1A_x_F21} = \text{cross}(R_{1A}, F21)$
 $\text{Dim } R_{2C\text{from}1_x_F12} \text{ As Array} = \text{cross}(R_{2C\text{from}1}, F12)$
 $\text{Dim } R_{2C\text{from}3_x_F32} \text{ As Array} = \text{cross}(R_{2C\text{from}3}, F32)$
 $\text{Dim } R_{3E_x_F23} \text{ As Array} = \text{cross}(R_{3E}, F23)$
 $\text{Dim } R_{4G_x_F54} \text{ As Array} = \text{cross}(R_{4G}, F54)$
 $\text{Dim } R_{5I\text{from}4_x_F45} \text{ As Array} = \text{cross}(R_{5I\text{from}4}, F45)$
 $\text{Dim } R_{5I\text{from}6_x_F65} \text{ As Array} = \text{cross}(R_{5I\text{from}6}, F65)$
 $\text{Dim } R_{6K_x_F56} \text{ As Array} = \text{cross}(R_{6K}, F56)$

* X and Y Force components on Bearing B

$Fy(1) = R_{1A_x_F21}(0, 0) / -(\text{BearingDistA} + \text{BearingDistB})$
 $Fx(1) = R_{1A_x_F21}(1, 0) / (\text{BearingDistA} + \text{BearingDistB})$

* X and Y Force components on Bearing D

$Fy(3) = (R_{2C\text{from}1_x_F12}(0, 0) + R_{2C\text{from}3_x_F32}(0, 0)) / -(\text{BearingDistA} + \text{BearingDistB})$
 $Fx(3) = (R_{2C\text{from}1_x_F12}(1, 0) + R_{2C\text{from}3_x_F32}(1, 0)) / (\text{BearingDistA} + \text{BearingDistB})$

* X and Y Force components on Bearing F

$Fy(5) = R_{3E_x_F23}(0, 0) / -(\text{BearingDistE} + \text{BearingDistF})$
 $Fx(5) = R_{3E_x_F23}(1, 0) / (\text{BearingDistE} + \text{BearingDistF})$

* X and Y Force components on Bearing H

$Fy(7) = R_{4G_x_F54}(0, 0) / -(\text{BearingDistG} + \text{BearingDistH})$
 $Fx(7) = R_{4G_x_F54}(1, 0) / (\text{BearingDistG} + \text{BearingDistH})$

* X and Y Force components on Bearing J

$Fy(9) = (R_{5I\text{from}4_x_F45}(0, 0) + R_{5I\text{from}6_x_F65}(0, 0)) / -(\text{BearingDistI} + \text{BearingDistJ})$
 $Fx(9) = (R_{5I\text{from}4_x_F45}(1, 0) + R_{5I\text{from}6_x_F65}(1, 0)) / (\text{BearingDistI} + \text{BearingDistJ})$

* X and Y Force components on Bearing L

$Fy(11) = R_{6K_x_F56}(0, 0) / -(\text{BearingDistK} + \text{BearingDistL})$
 $Fx(11) = R_{6K_x_F56}(1, 0) / (\text{BearingDistK} + \text{BearingDistL})$

* Solve for remaining components

* Bearing A

$Fx(0) = -F21(0, 0) - Fx(1)$
 $Fy(0) = -F21(1, 0) - Fy(1)$

* Bearing C

$Fx(2) = -F12(0, 0) - F32(0, 0) - Fx(3)$
 $Fy(2) = -F12(1, 0) - F32(1, 0) - Fy(3)$

* Bearing E

$Fx(4) = -F23(0, 0) - Fx(5)$
 $Fy(4) = -F23(1, 0) - Fy(5)$

* Bearing G

$Fx(6) = -F54(0, 0) - Fx(7)$
 $Fy(6) = -F54(1, 0) - Fy(7)$

* Bearing I

$Fx(8) = -F45(0, 0) - F65(0, 0) - Fx(9)$
 $Fy(8) = -F45(1, 0) - F65(1, 0) - Fy(9)$

* Bearing K

$Fx(10) = -F56(0, 0) - Fx(11)$
 $Fy(10) = -F56(1, 0) - Fy(11)$

```

' Thrust Loads

Fz(0) = F21(2, 0)
Fz(1) = F12(2, 0) + F32(2, 0)
Fz(2) = F23(2, 0)
Fz(3) = F54(2, 0)
Fz(4) = F45(2, 0) + F65(2, 0)
Fz(5) = F56(2, 0)

' Convert to forces on Bearings

For i = 0 To 11
    Fy(i) = -Fy(i)
    Fx(i) = -Fx(i)
Next

' Check to see if the user chose the 1G load option
If oneGLoadYes = True Then
    Fy(0) = Fy(0) - WeightA
    Fy(1) = Fy(1) - WeightB
    Fy(2) = Fy(2) - WeightC
    Fy(3) = Fy(3) - WeightD
    Fy(4) = Fy(4) - WeightE
    Fy(5) = Fy(5) - WeightF
    Fy(6) = Fy(6) - WeightG
    Fy(7) = Fy(7) - WeightH
    Fy(8) = Fy(8) - WeightI
    Fy(9) = Fy(9) - WeightJ
    Fy(10) = Fy(10) - WeightK
    Fy(11) = Fy(11) - WeightL
End If

' Calculate Resultant vectors and angles

For i = 0 To 11
    R(i) = Sqrt(Fy(i) ^ 2 + Fx(i) ^ 2)
    Angle_deg(i) = (Acos(Abs(Fy(i)) / R(i))) * 180 / pi
Next

' Convert Results back to SI if necessary
If SiChecked = True Then

    For i = 0 To 11
        Fx(i) = Fx(i) * 4.4482216
        Fy(i) = Fy(i) * 4.4482216
    Next

    For i = 0 To 5
        Fz(i) = Fz(i) * 4.4482216
    Next
End If

End Sub

```

Appendix C

Bearing Profile Plotting Program
MATLAB Code

```

% Bearing Profile Plotting Program
% Plots an Analytical solution adapted from Dr. Kirk's
% Manufacturing Tolerances Paper
%
% Written by Andy Wolff, Summer 2003

close all;
clear all;

% Define Parameters

degstep=.1; % Degree Step for Analytical solution

lobes=4;
rshaft=10; % Shaft Radius
Cp=8; % Lobe radial clearance
preload=.75;
rp=preload*Cp;
thetaL=0; % Angle to leading edge
alpha=1.14; % Offset
chi=90*pi/180; % Angular extent of Lobe
%Position of journal relative to bearing center
x=0;
y=0;
quadextent=[0:360/lobes:360];

% *****Analytical Solution*****

for quad=1:lobes
    htemp=0;
    count=0;
    for theta=0:degstep:quadextent(2)-degstep
        count=count+1;
        thetar=theta*pi/180;
        htemp(count)=Cp-rp*cos(thetaL + alpha*chi - thetar) - x*cos(thetar) - y*sin(thetar);
    end

    for count2=1:length([0:degstep:quadextent(2)-degstep])
        h(count2+(quadextent(quad))/degstep)=htemp(count2);
    end
end

% Add shaft diameter
h(length(h)+1)=h(1);
thetar=[0:degstep:360]*pi/180;
h=h+rshaft;

% Plot results
polar(thetar,h)
title(['Cp = ' num2str(Cp) ' mils; Preload = ' num2str(preload) ...
    ' ; chi = ' num2str(chi) ' ; offset = ' num2str(alpha)]);
hold on

%Plot Shaft
polar(thetar,rshaft*ones(size(h)),r)
hold on

% *****Measured Data from Bearing*****
%
load profiledata.mat;

newdata=profiledata(:,1:2);
h2=((newdata(2,:)-3.75)/2)*1000;
thetar=[0:5:360]*pi/180;

% Plot results
polar(thetar,fliplr(h2)+rshaft,'og')

```

Vita

Drs. David and Linda Wolff welcomed Andrew V. Wolff into the world on July 21, 1978 in Columbus, Ohio. After attending Walt Whitman High School in Bethesda, Maryland, Andrew traveled to upstate New York to attend Cornell University. In addition to his studies at Cornell, Andrew spent time on his own research projects and rowed on the varsity lightweight crew team. In the Summer of 2000, he received a Bachelor of Mechanical Engineering from Cornell University and accepted a job with General Electric Power Systems. General Electric trained Andrew for 8 months in Schenectady, New York to be a field engineer with expertise in steam turbine power generators. General Electric sent him to various power plants around the country while he was based out of Houston, Texas. During his 2 years with General Electric, Andrew gained installation and maintenance experience in gas and steam turbines as well as generators. In the Fall of 2002, Andrew was motivated to conduct research so he moved to Blacksburg, Virginia to begin a graduate level education at Virginia Polytechnic Institute and State University. In the Spring of 2004, he will receive his Master of Science in Mechanical Engineering from Virginia Polytechnic Institute and State University.